Geographical Fairness in Multi-RIS-Assisted Networks in Smart Cities: A Robust Design

Progress Zivuku, *Student Member, IEEE*, Abuzar B. M. Adam, *Member, IEEE*, Konstantinos Ntontin, *Member, IEEE*, Steven Kisseleff, *Senior Member, IEEE*, Vu Nguyen Ha, *Senior Member, IEEE*, Symeon Chatzinotas, *Fellow, IEEE* and Björn Ottersten, *Fellow, IEEE*

***Abstract*—In this work, we consider a typical scenario in a harsh urban propagation environment which is typical for a smart city scenario where multiple reconfigurable intelligent surfaces (RISs) are deployed in different hotspot areas to overcome signal blockage between the base station and users. Our goal is to ensure uninterrupted service availability to users in different hotspot areas regardless of their location. Consistent service availability can be achieved by guaranteeing that each RIS deployed in a hotspot area can support a certain number of users. This plays a critical role in smart city applications in the context of emergency communications and ubiquitous connectivity since the design ensures service availability to as many users as possible in all relevant locations. Taking into consideration the challenges in obtaining channel state information (CSI) given the passive nature of RIS and dynamic environments, we formulate a robust fairness problem to maximize the minimum expected number of served users in proximity to each RIS while considering the available transmit power and the worst-case quality of service (QoS) constraints within the bounded CSI error model framework. The resulting problem is a mixed integer non-convex program which is highly coupled and challenging to solve in polynomial time. Thus, we resort to binary variable relaxation, convex approximation techniques, and alternating optimization to tackle the problem. Additionally, we handle the semi-infinite uncertainty constraints by employing the S-procedure and general sign-definiteness. Simulation results demonstrate the effectiveness of the proposed design in obtaining consistent and reliable service in different hotspot areas compared to the relevant benchmark schemes. In addition, the proposed design shows flexibility in serving users with their target QoS given different channel uncertainty levels.**

***Index Terms*—Reconfigurable intelligent surfaces, Resource allocation, User association, Smart cities, Quality of service, Precoding, Geographical fairness, Successive convex approximation, Robust optimization, S-procedure.**

I. Introduction

A. Background

Future generations of wireless networks are envisioned to provide seamless connectivity and to support the ever-increasing number of connected devices [2], [3]. The provision of seamless connectivity will be highly instrumental in smart cities for supporting a wide range of services and effectively satisfying user demands. Note that smart city applications involve an exchange of critical and sensitive information under system constraints [4]. Essential services, such as government, emergency services, and healthcare, may require prompt service availability. Consequently, telecom operators bear the responsibility of ensuring consistent service availability across the majority of locations within the city. Additionally, these urban areas should leverage cutting-edge technologies to streamline resource utilization, promote sustainability, and enhance the overall well-being of residents [5]. In recent years, there has been a growing interest in the study of reconfigurable intelligent surfaces (RISs) and their deployment in smart cities to enhance public service accessibility, promote the digitization of urban spaces, and monitor various societal processes and city assets [4]. A RIS refers to a software-defined meta surface equipped with the capability to enhance wireless network performance by adjusting the reflection of the impinging electromagnetic signals towards the intended destination [6]–[9]. The deployment of RIS is quite promising for future generations of wireless networks due to its potential to reduce power consumption as compared to traditional relay networks (e.g. amplify and forward and decode and forward relays) [10]–[12]. Additionally, RIS deployment extends coverage to areas where there is no line of sight (LOS) path or where the direct connection between the base station (BS) and users is obstructed [13]. In this context, the deployment of multiple RISs is primarily envisioned in urban areas (e.g., smart cities) for coverage extension to blindspots caused by blockages from city infrastructure [4]. This is expected to advance the realization of smart radio environments which will be highly beneficial in smart cities for seamless connectivity and enhancement of energy and spectral efficiencies [14]–[16]. Moreover, RIS deployment may result in reduced exposure to electromagnetic waves to citizens which supports the idea of sustainable, green environments in smart cities [4].

Current research on RIS-assisted networks focused on the joint optimization of active and passive beamforming (BF) for various system configurations [17]–[19]. The work in [20], studied the performance of joint symbol level precoding and RIS phase shift design for power minimization. In [21], the authors demonstrated the advantages of RIS-based communications in maximizing energy efficiency in comparison to deploying regular multi-antenna amplify-and-forward relaying. RIS-assisted communications have shown to be highly instru-

This work is funded by the Luxembourg National Research Fund (FNR) as part of the CORE program under project RISOTTI C20/IS/14773976 and in part by FNR under Grant INTER/MOBILITY/2023/IS/18014377/MCR. An earlier version of this work was presented in part at the IEEE ICC 2024 conference in Denver, CO, USA, 9-13 June 2024 [1].

Progress Zivuku, Abuzar B. M. Adam, Konstantinos Ntontin, Vu Nguyen Ha, Symeon Chatzinotas and Björn Ottersten are with the Interdisciplinary Centre for Security, Reliability and Trust (SnT), University of Luxembourg (E-mails: {progress.zivuku, abuzar.babikir, kostantinos.ntontin, vu-nguyen.ha, symeon.chatzinotas, bjorn.ottersten }@uni.lu).

Steven Kisseleff is with the Fraunhofer Institute for Integrated Circuits IIS, Germany (E-mail: steven.kisseleff@iis.fraunhofer.de).

This article has been accepted for publication in IEEE Transactions on Communications. This is the author's version which has not been fully edited and content may change prior to final publication. Citation information: DOI 10.1109/TCOMM.2025.3525568

Fig. 1: Smart city scenario with hotspot areas supported by distributed RISs.

mental in sum-rate maximization as demonstrated in [22]–[25]. Further, the application of RIS has been shown to significantly improve the number of served users [26], [27]. This is mainly because, in certain scenarios, most signals go through the RIS. However, the works outlined above considered the availability of perfect instantaneous channel state information (CSI) in their design.

Practically, due to the passive nature of the RIS and the dynamic environments, perfect CSI is highly challenging to obtain [28]–[31]. In this context, the study in [32] developed robust BF techniques aimed at minimizing power consumption, taking into account imperfect CSI for the RIS-user link. The authors argued that the BS-user link can be obtained with high accuracy via conventional channel estimation techniques e.g. the least square algorithm. Additionally, the indirect link from the BS-RIS can be derived by computing the angles of arrival and departure which exhibit minimal variation due to the fixed positions of both the RIS and the BS. Further, the study in [33] investigated a robust transceiver design for a multi-RIS network taking into consideration channel estimation errors on each hop of the RIS links. However, implementing this approach in practice is challenging due to the limited signal processing capability of passive RISs or standard reflective-only RISs. This approach requires active elements to be installed at the RIS to estimate the individual channels [34], potentially increasing hardware costs and power consumption. Further, this may also result in higher information exchange overhead since the estimated channel information at the RIS must be fed back to the BS. In response to these challenges, authors in [35] designed a framework for robust optimization design in RIS-assisted networks. Practically, it is more feasible to consider the cascaded channel uncertainty in RIS-assisted wireless communication systems [1].

Note that most of the aforementioned works primarily focused on designs involving a single RIS. However, in practice, the BS may be assisted by multiple RISs. Specifically, the deployment of multiple RISs will, in general, be required in harsh propagation environments as is expected in urban areas. In this context, several authors studied the benefits of deploying distributed RISs for sum rate maximization, energy efficiency maximization, signal-to-leakage-and-noise ratio (SLNR) maximization, and max-min signal-to-interference plus noise ratio (SINR) [37]–[41]. Specifically, in [42] and [43], a typical weighted sum-rate maximization problem was examined for a multiple-RIS-assisted system, considering both ideal and non-ideal hardware scenarios. Further, the authors in [44] and [45] focused on the statistical characterization and performance analysis of systems supported by multiple RISs, theoretically deriving the ergodic achievable rate for cooperative RISs under Rician fading and Nakagami-m fading, respectively. In [46], a weighted sum-rate maximization problem for a multi-hop RIS-aided system was studied. Simulation results demonstrated the performance gain improvements obtained through the deployment of multiple RISs in the network. Beyond these studies, the potential of RISs to enhance energy efficiency has also been explored in [37]. The authors aimed to maximize the energy efficiency of a wireless network utilizing multiple RISs by optimizing the RIS reflection coefficients and dynamically managing the on-off status of each RIS.

B. Motivation and contribution

1) Motivation: According to the literature mentioned in the previous section, several works focused on sum rate maximization, power minimization and energy efficiency maximization in RIS-assisted networks [37]–[39], [41]–[47]. Additionally, to ensure fairness, previous studies focused on maximizing the minimum achievable data rate or the SINR of the user [39], [40]. Although these formulations are quite useful from a system design perspective, none of them can guarantee a fair and consistent service to users in various hotspot areas supported by distributed RISs. Further, these commonly considered objective functions do not guarantee that users are served with their desired quality of service (QoS) which is a more service-oriented approach and is highly beneficial in the concept of smart cities. Specifically, serving users with their desired QoS is favorable in smart cities where various

[1]Note that channel estimation for the cascaded channel has been intensively studied in RIS-aided multiple-input multiple-output (MIMO) systems [36].

Works	Objective Function	Number of RIS	Robust Optimization Design	Geographical Fairness	User Admission Control	User QoS Assurance
[41], [46]	Sum-rate maximization	Multiple	✗	✗	✗	✗
[32], [35]	Power minimization	Single	✓	✗	✗	✗
[37]	Energy efficiency maximization	Multiple	✗	✗	✗	✗
[39], [40]	Max-min SINR/Rate	Multiple	✗	✗	✗	✗
[26], [27]	User admission maximization	Single	✗	✗	✓	✓
This work	Max-min number of served users per RIS	Multiple	✓	✓	✓	✓

TABLE I: Comparison of our work with existing related works

applications function with different QoS requirements. It is also important to note that ensuring the desired QoS is strongly justified for voice, streaming media, and other interactive applications, and it remains the dominant design strategy in cellular wireless networks today [48].

Next, ensuring fair resource utilization and load balancing in multi-RIS-assisted networks is highly challenging. This is crucial to ensure that there is no load imbalance where some RIS elements are overloaded while the others are underloaded especially when the RIS panels are identical [49].

Besides, it is important to highlight that previous work in conventional networks without RIS highlighted the importance of supporting as many users as possible at their desired QoS [50]. Further, the authors in [51] studied the max-min fair resource allocation problem to ensure fairness among several groups of vehicle to everything (V2X) users. In addition, studies in [27] demonstrated the advantages of RIS for user admission maximization in a single RIS-assisted network. Nevertheless, we note that maximizing the total number of served users in a multi-RIS-assisted network may lead to inconsistent service in different locations or hotspot areas. Note that the findings of investigations from previous studies demonstrated that RISs are usually deployed close to the users for better performance [52]. Accordingly, RISs are practically useful for creating ”signal hotspots” and serving users in their vicinity. In this context, RISs can be deployed separately in different geographical locations to provide robust data transmission. This approach stands out as a practical and effective solution for enhancing service coverage and optimizing wireless communication networks. However, the dense deployment of RISs necessitates advanced resource allocation techniques for improved network resource efficiency. Specifically, advanced resource allocation techniques are required to address the unique challenges posed by multi-RIS-aided networks [53]. For instance, in scenarios where the RISs are deployed in a distributed manner, the BS may have preferred channels or RISs to serve a group of users due to different channel conditions. Thus, the users close to the RIS with unfavorable channel conditions will be out of coverage resulting in coverage holes/ blind spots. This is unfair because certain locations will be preferred to serve more users over other locations. Additionally, in case of unfair geographical locations, the service can become unavailable in some hotspot areas. Specifically, depending on the link quality only the users in one hotspot (close to one RIS) may be supported while the users in other locations may be neglected. Consequently, the service provider can lose customers in some locations if users always experience a drop in performance. This is not aligned with the future of modern telecommunications which is to provide seamless connectivity or uninterrupted service irrespective of the geographical location of users. In this case, ensuring service availability in hotspot areas like parks, shops, outdoor event grounds, city streets, and bus stops, without being hindered by location constraints becomes an important design criterion. Specifically, it is important to ensure reliable connectivity to as many users as possible in all relevant locations, which is crucial in the context of emergency communication and ubiquitous connectivity.

On the other hand, we note that with imperfect CSI, it is highly challenging to serve users with their desired QoS [26]. The performance of RIS-assisted communication systems is heavily reliant on the presence of accurate CSI. However, the assumption of accurate CSI in multi-RIS-assisted networks may not always be practical. Specifically, the BS might only have access to incomplete or outdated CSI in situations with high mobility and rapidly changing channel conditions. This can result in signal misalignment. Consequently, exploring robust BF design that considers imperfect CSI in optimization problems is required.

2) Contribution: Due to the aforementioned limitations of the current literature, in this work, we consider a typical scenario in a smart city where multiple RISs are deployed on billboards to extend coverage to different hotspot areas, as depicted in Fig. 1. This represents real-world scenarios in urban environments, e.g. smart cities, where RISs are deployed to improve the performance of the communication system by customizing the propagation of the radio waves impinging upon them, thereby enabling cost-and energy-efficient signal transmission [14]. The scenario depicted in Fig. 1 draws inspiration from advancements in smart city initiatives highlighted in prior studies, aiming to enhance connectivity and optimize the overall functionality of smart cities [4], [54]–[57]. Furthermore, the scenario supports the vision of future generations of wireless networks to enable a seamless and ubiquitous experience, and service continuity, considering efficiency and affordability [58] [59]. In addition, it aligns with the envisioned sustainable development goals, where the adoption of green technologies is a key design criterion in future wireless networks [58].

In smart cities, ubiquitous connectivity and immediate service availability are vital for the seamless operation of applications like traffic management, public safety, and environmental monitoring. Telecom operators must ensure reliable coverage across all areas, prioritizing fairness among user groups in various zones to guarantee equitable access to services. This is essential for real-time data processing, consistent quality, and public safety during emergencies. As smart cities grow, networks must be scalable, resilient, and capable of delivering

fair, consistent service across all regions to support future innovations [60], [61].

Our main goal in this work is to provide geographically fair access service to users in smart cities, a critical aspect in the context of emergency communication and ubiquitous connectivity. Additionally, we aim to jointly optimize the precoding at the BS and BF at RISs to ensure stable system performance, focusing on maintaining fairness among different user groups across various geographic zones within the city. Specifically, we propose a robust optimization framework to maximize the minimum number of users served at their target QoS near each RIS. The proposed design ensures that every RIS in the network supports a designated number of users. This approach is essential for enabling a broad range of emergency services to operate effectively and deliver assistance across diverse geographical areas. Enhanced service availability and reliability across diverse locations are vital for maintaining uninterrupted service delivery for critical applications such as online banking and business communications. In modern telecommunication systems, user satisfaction relies heavily on consistent QoS, where service continuity is prioritized over peak performance. Therefore, the primary goal of future mobile networks should not solely focus on increasing peak rates but rather on ensuring consistent rates for the vast majority of locations within their coverage area [62], [63]. Furthermore, this design enables users to be served according to their specific QoS requirements, accommodating varying QoS needs. The contributions and novelty of this work, in comparison to the existing literature, are detailed in TABLE I.

Introducing a robust and geographically fair access design for smart cities, ensuring stable service delivery across various zones, the key contributions of this work are summarized in the following.

- For a smart city scenario where the BS supports multiple hotspots through distributed RISs, we formulate and provide a solution to the resource allocation problem to guarantee geographical fairness in terms of the number of users served by each RIS in different locations. It is important to note that the users' geographical location is closely tied to the RIS, meaning that users are served by their closest RIS. In particular, we aim to provide fair coverage and load balancing between the distributed RISs. To achieve geographical fairness, we formulate two optimization problems: the first under a perfect CSI assumption (non-robust design) and the second under an imperfect CSI assumption (robust design), corresponding to the serving of users in indoor and outdoor scenarios, respectively. The objective is to maximize the minimum expected number of users achieving their target QoS in proximity to each RIS while considering the available total transmit power at the BS and the worst-case QoS constraints[2]. This approach ensures efficient operation of a wide range of emergency services and service availability for users in high-traffic areas, such as shops, smart city streets, and bus stops. To the best of our knowledge, this is the first attempt to design robust optimization for geographical fairness in RIS-assisted wireless networks. The robust max-min fairness design is essential since obtaining perfect instantaneous CSI in RIS-assisted networks is highly challenging. The design ensures stable system performance, even under the most challenging conditions.
- The problem outlined above is a mixed integer non-linear program (MINLP), known to be NP-hard [64]. Thus, computing its globally optimal solution is highly challenging and computationally expensive. The constraints in the problem are highly coupled, which makes it difficult to address using conventional convex optimization techniques. In addition, due to the CSI uncertainty continuity, the QoS constraint involves semi-infinite non-convex inequality constraints. To address the complex robust optimization problem, we propose a simple yet effective iterative algorithm. The proposed algorithm integrates alternating optimization (AO), convex approximations, mathematical transformations, the S-procedure, and general sign-definiteness to ensure convergence to at least a locally optimal solution. Firstly, we relax the binary constraint to a box constraint and then penalize the objective function to ensure binary solutions at convergence. Next, we resort to AO to decouple the problem into two manageable sub-problems. Lastly, the non-convexity of these sub-problems is tackled through the use of convex approximations, mathematical transformations, the S-procedure, and general sign-definiteness techniques.
- Simulation results demonstrate the performance gain of the proposed design against relevant benchmark schemes. Further, we provide insights on the performance of the proposed design compared to the max-sum design where the total number of served users is maximized without considering fairness. In this case, we demonstrate the significance of having consistent and reliable service availability across various hotspot areas supported by distributed RISs. In addition, we show the flexibility provided by the proposed design in serving users with their desired QoS given different channel uncertainty levels.

The rest of the paper is organized as follows. Section II introduces the system model. In Section III we formulate two optimization problems for a multi-RIS-assisted wireless network considering the case of perfect and imperfect CSI. We first formulate the non-robust max-min fairness design where perfect instantaneous CSI is considered available at the BS. Next, we extend the non-robust design to a robust max-min fairness design in the presence of imperfect CSI within the framework of the bounded CSI error model. In Section IV, we propose an AO algorithm based on successive convex approximation (SCA), the S-procedure, and general sign-definiteness to solve the formulated robust max-min fairness problem. Additionally, we provide a detailed derivation of the proposed solution. Section V presents the numerical results to evaluate the performance of the proposed design. Finally, we

[2]We note that the consideration of the imperfect CSI case and the robust proposed design constitutes an extension of the non-robust design under perfect CSI that is considered in [1].

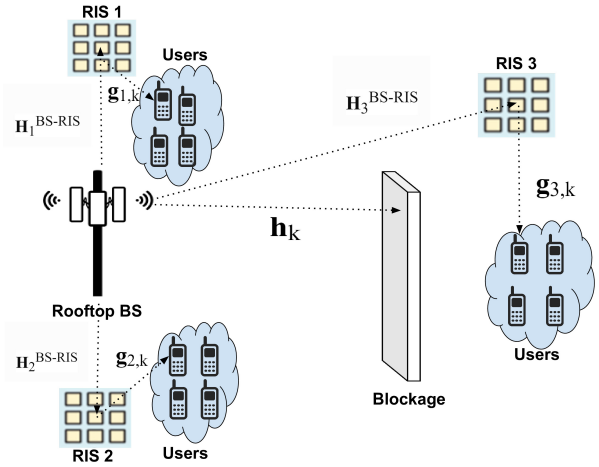

Fig. 2: Multi-RIS-aided multi-user MISO system.

conclude the paper in Section VI.

Notations: Scalars are denoted by italic letters, vectors and matrices are denoted by bold-face lower-case and upper-case letters, respectively. $\mathbb{C}^{x\times y}$ denotes the space of $x\times y$ complex-valued matrices. $\mathrm{Tr}\{\cdot\}, |\cdot|, ||\cdot||, (\cdot)^*, (\cdot)^H, (\cdot)^T, \mathrm{Re}\{\cdot\}$ and $\arg(\cdot)$ denote the trace of a complex number, absolute value, Euclidean norm, conjugate, Hermitian transpose, transpose, real part and the phase, respectively. diag(.) produces a square matrix with the elements of its argument on the main diagonal and zeros otherwise. $\boldsymbol{A}\otimes\boldsymbol{B}$ denotes the Kronecker product between matrix $\boldsymbol{A}$ and $\boldsymbol{B}$. $\boldsymbol{A}\succeq\boldsymbol{B}$ denotes that the difference between matrix $\boldsymbol{A}$ and matrix $\boldsymbol{B}$ is a positive semidefinite.

II. System Model

We consider a multi-RIS-assisted multi-user multiple-input single-output (MISO) system, depicted in Fig. 2. In this setup, a BS, equipped with M antennas, communicates with K single-antenna users in various hotspots via L distributed RISs, each equipped with N reflective elements[3]. Hereafter, one denotes $\mathcal{K}$ and $\mathcal{L}$ as the sets of all K users and L RISs, respectively. Let $\boldsymbol{\theta}_\ell\in\mathbb{C}^{N\times 1}$ be the phase shift vector induced by the RIS ℓ where $\boldsymbol{\Theta}_\ell$=diag$([e^{j\theta_{1,\ell}}\dots e^{j\theta_{n,\ell}}\dots e^{j\theta_{N,\ell}}])$ is the diagonal matrix that captures the reflective properties of the RIS[4]. We consider a linear precoding design at the BS, where the k-th user is assigned a dedicated BF vector $\mathbf{w}_k\in\mathbb{C}^{M\times 1}$. The complex baseband signal at the BS can be expressed as $\mathbf{x}=\sum_{k\in\mathcal{K}}\mathbf{w}_k s_k$, where s_k denotes the data symbol intended to user k, which is assumed to have zero mean and unit variance.

In this case, s_k is assumed independent and identically distributed (i.i.d) across K users. Accordingly, the total transmit power at the BS is

$$P^{\text{total}}=\sum_{k\in\mathcal{K}}||\mathbf{w}_k||^2. \tag{1}$$

[3]We highlight that RISs can be implemented in diverse ways including simultaneously transmitting and reflecting RIS (STAR-RISs) [65]. However, the study of STAR-RIS deployment and its benefits to the considered design is beyond the scope of this work.

[4]We assume a centralized controller (e.g., at the base station) that coordinates the phase shifts of each RIS based on CSI [15].

In this work, double-RIS reflections are assumed to be negligible due to the pathloss scaling associated with the product of distances between the RISs, given significant separation distances in realistic settings, as well as their geometrical orientation [37]. Moreover, we assume that signal reflections from other RISs deployed in separate hotspot areas are negligible, owing to the specific orientation of the proposed scenario in Fig. 1. Additionally, in harsh urban environments, signal reflections from distant RISs are more likely to be obstructed by city infrastructure. In this context, the localized coverage of passive RISs proves highly effective in simplifying inter-RIS interference management, as the RISs are appropriately spaced apart. It is important to note that we assume a targeted deployment of RISs in specific, high-impact areas, where the distances between RISs are sufficiently large. This deployment strategy is both practical and cost-effective in the near term, allowing network operators to maximize the advantages of RIS technology while managing costs and system complexity. Note that an alternative approach would involve joint transmission, which, however, introduces significant channel estimation overhead due to the need to estimate cross-interference channels for all RISs and users in different hotspot areas. This would require more resources for channel estimation, leading to increased system complexity, reduced performance, and longer processing times.

The BS-RIS ℓ, BS-user k, and RIS ℓ-user k channels are denoted as $\mathbf{H}_\ell^{\text{BS}-\text{RIS}}\in\mathbb{C}^{N\times M}$, $\mathbf{h}_k\in\mathbb{C}^{M\times 1}$, and $\mathbf{g}_{\ell,k}\in\mathbb{C}^{N\times 1}$, respectively. To achieve geographical fairness, the RIS-user association is obtained prior to optimization. In this case, geographical fairness is directly linked to serving users in close proximity to the RIS since the RISs are deployed to serve users in hotspot areas. Correspondingly, to achieve geographical fairness in terms of RIS-user association, user k associated to RIS ℓ is selected based on the minimum distance criteria as follows

$$\{k,\ell\}=\arg\min(d_{\ell,k}),\forall\ell\in\mathcal{L},\forall k\in\mathcal{K}, \tag{2}$$

where $d_{\ell,k}$ is the distance between RIS ℓ and user k. In this context, we denote the RIS ℓ to user k association with the variable $\psi_{k,\ell}$. This can be represented as follows

$$\psi_{k,\ell}=\begin{cases}1, & \text{if user } k \text{ is associated to RIS } \ell;\\ 0, & \text{otherwise.}\end{cases} \tag{3}$$

Here, $\boldsymbol{\psi}_\ell\triangleq[\psi_{k,\ell}]_{k\in\mathcal{K}}$ is a vector denoting the association state of RIS ℓ to all the users, where $\boldsymbol{\psi}\triangleq[\boldsymbol{\psi}_\ell]_{\ell\in\mathcal{L}}$ is the RIS-user association matrix.

Next, the received signal at user k is given by

$$y_k=\Big[\mathbf{h}_k^H+\sum_{\ell\in\mathcal{L}}\psi_{k,\ell}(\mathbf{g}_{\ell,k}^H\boldsymbol{\Theta}_\ell\mathbf{H}_\ell^{\text{BS}-\text{RIS}})\Big]\sum_{i\in\mathcal{K}}\mathbf{w}_i s_i+v_k, \tag{4}$$

where v_k is the additive white Gaussian noise (AWGN) at user k with zero mean and variance σ_k^2, i.e. $n_k[\ell]\sim\mathcal{CN}(0,\sigma_k^2)$. The instantaneous received SINR at user k is denoted by

$$\gamma_k(\mathbf{W},\boldsymbol{\Theta})=$$

$$\frac{\left|\left[\mathbf{h}_k^H + \sum_{\ell\in\mathcal{L}} \psi_{k,\ell}(\mathbf{g}_{\ell,k}^H \boldsymbol{\Theta}_\ell \mathbf{H}_\ell^{\mathrm{BS-RIS}})\right]\mathbf{w}_k\right|^2}{\sum\limits_{i\in\mathcal{K}/\{k\}} \left|\left[\mathbf{h}_k^H + \sum\limits_{\ell\in\mathcal{L}} \psi_{k,\ell}(\mathbf{g}_{\ell,k}^H \boldsymbol{\Theta}_\ell \mathbf{H}_\ell^{\mathrm{BS-RIS}})\right]\mathbf{w}_i\right|^2 + \sigma_k^2}, \tag{5}$$

where $\mathbf{W} \triangleq [\mathbf{w}_k]_{k\in\mathcal{K}}$ is a matrix that contains all the precoding vectors for all users. Additionally, $\boldsymbol{\theta} \triangleq [\boldsymbol{\theta}_\ell]_{\ell\in\mathcal{L}}$ is a matrix that contains all the phase shift vectors for all RISs and $\boldsymbol{\Theta} = [\boldsymbol{\Theta}_\ell]_{\ell\in\mathcal{L}}$ contains the diagonal matrices with the reflective properties of all the RISs.

III. Problem Formulation

To formulate the optimization problem under consideration, we introduce a binary variable a_k to determine the set of served users, i.e., the users that can achieve their target QoS,

$$a_k = \begin{cases} 1, & \text{if user } k \text{ is served with } \gamma_k \geq \Gamma_k^{\mathrm{th}}; \\ 0, & \text{otherwise.} \end{cases} \tag{6}$$

where Γ_k^{th} is the required SINR for user k to satisfy the QoS requirements. Let $\boldsymbol{a} \triangleq [a_k]_{k\in\mathcal{K}}$ be a user-satisfactory stage vector. Specifically, a user is considered well-served if it satisfies the required QoS. This can be represented as $\gamma_k \geq a_k\Gamma_k^{\mathrm{th}}$, where $a_k \in \{0,1\}$. If $a_k = 1$, it is equivalent to $\gamma_k \geq \Gamma_k^{\mathrm{th}}$, i.e., the user is well-served and receives its desired SINR. Otherwise, $a_k\Gamma_k$ reduces to zero and the constraint is disabled. Note that being associated with RIS ℓ does not guarantee that the user is well-served.

Remark 1. *Note that a_k is a binary indicator to determine the state of each user i.e., whether the user is well-served or not. Similarly, $\psi_{k,\ell}$ is another binary variable indicating the association of user k to RIS ℓ. Here, $\boldsymbol{\psi}_\ell \triangleq [\psi_{k,\ell}]_{k\in\mathcal{K}}$ is a vector denoting the association state of RIS ℓ to all the users, where $\boldsymbol{\psi} \triangleq [\boldsymbol{\psi}_\ell]_{\ell\in\mathcal{L}}$ is the RIS-user association matrix. In this work, geographical fairness refers to ensuring equitable access to services by prioritizing users located near the RIS, while also maintaining service balancing across different geographical zones within the network. To do so, we aim to optimize a product of the RIS-user association matrix $\boldsymbol{\psi}$ and the user satisfactory vector $\boldsymbol{a}$ to maximize the minimum expected number of well-served users in each hotspot area. Here, the association between the RISs and the users is predetermined according to the geographical location. Accordingly, the objective function can be represented as $\max \min_{\ell\in\mathcal{L}}(\boldsymbol{\psi}_\ell^T \boldsymbol{a})$. In this case, $\boldsymbol{\psi}_\ell^T \boldsymbol{a}$ represents the number of well-served users by the ℓ-th RIS or in a specific hotspot area. This guarantees that no hot spot area is disproportionately underserved, promoting fairness across geographical areas supported by the distributed RISs*[5].

[5]It is important to note that consistent service availability is widely characterized by minimizing the outage probability [66]. However, in this work, we consider a user-centric approach that mitigates the risk of service unavailability in certain hotspot areas, allowing the scheduling of as many users as possible independently of their locations under the maximum available transmit power and the worst-case QoS constraints.

A. Perfect Instantaneous CSI

Firstly, we formulate the non-robust optimization problem to maximize the minimum number of well-served users in proximity to each RIS subject to total available power at the BS and the QoS constraints as follows,

$$\max_{\boldsymbol{\Theta},\mathbf{W},\boldsymbol{a}} \min_{\ell\in\mathcal{L}} \boldsymbol{\psi}_\ell^T \boldsymbol{a} \tag{7a}$$

$$\text{s. t.} \quad \gamma_k(\mathbf{W},\boldsymbol{\Theta}) \geq a_k\Gamma_k^{\mathrm{th}}, \forall k \in \mathcal{K}, \tag{7b}$$

$$\sum_{k\in\mathcal{K}} \|\mathbf{w}_k\|^2 \leq P^{\max}, \tag{7c}$$

$$\|\mathbf{w}_k\|^2 \leq a_k P^{\max}, \forall k \in \mathcal{K}, \tag{7d}$$

$$0 \leq \theta_{n,\ell} \leq 2\pi, \ \forall n \in \mathcal{N}, \forall \ell \in \mathcal{L}, \tag{7e}$$

$$a_k \in \{0,1\}, \ \forall k \in \mathcal{K}, \tag{7f}$$

where $\mathcal{N} = \{1,...,N\}$ and $\boldsymbol{\Gamma} \triangleq [\Gamma_k^{\mathrm{th}}]_{k\in\mathcal{K}}$ is a vector that contains the QoS requirements of each user. The constraints in problem (7) are explained in detail as follows:

- Constraint (7b) ensures that every well-served user in a geographical area satisfies its required minimum QoS.
- Constraint (7c) implies the transmission power budget limitation at the BS.
- For efficient resource utilization, constraint (7d) ensures that power is only allocated to well-served users. In this case, the precoding vector $\mathbf{w}_k$ is equal to zero for a user k that is not well-served.
- Constraint (7e) ensures that the phase shifts of all RIS elements are between 0 and 2π.
- Constraint (7f) remarks the user satisfactory stage in (6).

Problem (7) can be solved via SCA-based AO algorithm [1]. This design corresponds to scenarios where the CSI can be assumed to be perfect e.g. the outdoor-to-indoor scenarios. The availability of perfect CSI in these scenarios can be justified by the slow mobility of users inside the target buildings [1]. However, for outdoor scenarios, the CSI may be imperfect or outdated due to user mobility. As a result, we focus on the robust resource allocation design in the presence of imperfect CSI in the next subsection.

B. Robust Design with Imperfect CSI

1) Imperfect Estimated CSI Model: Towards formulating the robust max-min fairness design, we denote the cascaded channel matrix from the BS to user k through RIS ℓ as $\mathbf{H}_{\ell,k} = \mathrm{diag}(\mathbf{g}_{\ell,k}^H)\mathbf{H}_\ell^{\mathrm{BS-RIS}}$, where $\mathbf{H}_{\ell,k} \in \mathbb{C}^{N\times M}$. In this scenario, the estimated cascaded channel matrix is considered imperfect due to the mobility of users in outdoor environments. However, we assume that the direct link, if available, can be accurately estimated using conventional channel estimation methods, such as the least squares algorithm [32]. The cascaded channel $\mathbf{H}_{\ell,k}$ is considered imperfect, therefore, we present it as $\mathbf{H}_{\ell,k} = \hat{\mathbf{H}}_{\ell,k} + \boldsymbol{\Psi}_{\ell,k}$, where $\hat{\mathbf{H}}_{\ell,k} \in \mathbb{C}^{N\times M}$ is the estimated cascaded channel matrix which is known at the BS, and $\boldsymbol{\Psi}_{\ell,k} \in \mathbb{C}^{N\times M}$ represents the unknown estimation error matrix. For simplicity we let, $\hat{\mathbf{H}}_k = \sum_{\ell\in\mathcal{L}} \psi_{\ell,k}\hat{\mathbf{H}}_{\ell,k}$ and $\boldsymbol{\Psi}_k = \sum_{\ell\in\mathcal{L}} \psi_{\ell,k}\boldsymbol{\Psi}_{\ell,k}$ which denote the estimated channel and estimation error matrices corresponding to user k, respectively. One may need to recall that each user is assisted by the RIS

closest to it. In this context, every user can be associated with, i.e., be assisted by, only one pre-determined RIS. Note that a norm-bounded error model studied in [67] is employed in this work. This can be motivated for outdoor scenarios, where the users have a maximum velocity they can drive or walk with. Specifically, this is reasonable inside urban areas where there are speed limits or in cases of pedestrians walking on the city streets. In such scenarios, the mobility of users or objects is predictable (e.g., vehicles on a highway with known speeds and directions), and channel variations can be anticipated. Hence, a bounded user velocity would translate to a bounded channel error model in such a case. Predictable or known mobility patterns in smart cities allow estimation errors to be bounded. Accordingly, the bounded error is denoted as[6]

$$\|\mathbf{\Psi}_k\| \leq \zeta_k, \forall k \in \mathcal{K}, \tag{8}$$

where $\|*\|$ stands for the norm-2 operation of a matrix, and ζ_k denotes the radii of the uncertainty region which can be estimated at the BS based on the stochastic analysis [35].

2) Imperfect-CSI Robust Problem Formulation: Regarding RIS ℓ's phases ($\forall \ell \in \mathcal{L}$), let $\boldsymbol{\phi}_\ell$ be the diagonal elements of the matrix $\mathbf{\Theta}$ for RIS ℓ where $\boldsymbol{\phi}_\ell = [\phi_{1,\ell}, \cdots, \phi_{n,\ell}, \cdots, \phi_{N,\ell}] \in \mathbb{C}^{N\times 1}$ and $\phi_{n,\ell} = e^{j\theta_{n,\ell}}$. Then, one further denotes $\boldsymbol{\phi} = [\boldsymbol{\phi}_\ell]_{\ell\in\mathcal{L}} \in \mathbb{C}^{N\times L}$ as the passive BF matrix with the phases for all distributed RISs. Accordingly, we formulate a robust design to maximize the minimum number of well-served users in proximity to each RIS subject to total available power at the BS and the worst-case SINR constraints under the norm-bounded CSI error model as follows

$$\max_{\boldsymbol{\phi},\mathbf{W},\boldsymbol{a}} \ \min_{\ell\in\mathcal{L}} \ \boldsymbol{\psi}_\ell^T \boldsymbol{a} \tag{9a}$$

$$\text{s. t.} \quad \gamma_k(\mathbf{W},\boldsymbol{\phi}) \geq a_k \Gamma_k^{\text{th}}, \forall \|\mathbf{\Psi}_k\| \leq \zeta_k, \forall k \in \mathcal{K}, \tag{9b}$$

$$\sum_{k\in\mathcal{K}} \|\mathbf{w}_k\|^2 \leq P^{\max}, \tag{9c}$$

$$\|\mathbf{w}_k\|^2 \leq a_k P^{\max}, \forall k \in \mathcal{K}, \tag{9d}$$

$$|\boldsymbol{\phi}_{n,l}| = 1, \ \forall n \in \mathcal{N}, \forall \ell \in \mathcal{L}, \tag{9e}$$

$$a_k \in \{0,1\}, \ \forall k \in \mathcal{K}, \tag{9f}$$

where

$$\gamma_k(\mathbf{W},\boldsymbol{\phi}) = \frac{\left|\left(\mathbf{h}_k^{\mathrm{H}} + \sum_{\ell\in\mathcal{L}} \psi_{\ell,k} \boldsymbol{\phi}_\ell^{\mathrm{H}} \mathbf{H}_{\ell,k}\right) \mathbf{w}_k\right|^2}{\sum\limits_{i\in\mathcal{K}/\{k\}} \left|\left(\mathbf{h}_k^{\mathrm{H}} + \sum_{\ell\in\mathcal{L}} \psi_{\ell,k} \boldsymbol{\phi}_\ell^{\mathrm{H}} \mathbf{H}_{\ell,k}\right) \mathbf{w}_i\right|^2 + \sigma_k^2}. \tag{10}$$

Herein, constraints (9c), (9d), and (9f) are formulated similarly to (7c), (7d), and(7f), respectively. Below we explain in detail the remaining constraints

- Constraint (9b) is designed such that the well-served users in different hotspot areas can achieve their target SINRs for all channel error realizations.
- Constraint (9e) is the unit modulus constraint for the RIS phase-shift design.

[6]It is important to note that the norm bounded channel error model in this work is used as a design parameter to robustify the optimization design solution. In this scenario, the model aims to ensure system performance remains stable even in the most adverse conditions.

3) Nature of the Formulated Problem: As can be seen, problem (9) is a mixed integer non-convex problem known to be NP-hard. Specifically, the problem is classified as a MINLP due to the coupling of the optimization variables $\boldsymbol{\phi}$, and $\mathbf{W}$ in constraint (9b), the unit modulus constraint in (9e) and the binary variable in constraint (9f). Additionally, due to the CSI uncertainty continuity, the SINR (QoS) constraint (9b) has semi-infinite non-convex inequality constraints. Further, it is important to note that the objective function in (9a) is non-smooth. These factors make problem (9) highly challenging to solve using standard convex optimization methods. As a result, solving this problem via combinatorial programming or convex optimization techniques is extremely difficult, and finding a globally optimal solution within polynomial time may not be feasible.

4) Solution Approach: To address the challenging robust optimization problem (9), we propose a simple yet efficient iterative AO algorithm, convex approximations, mathematical transformations, the S-procedure, and general sign-definiteness. The algorithm guarantees convergence to at least a locally optimal solution. Specifically, we first relax the binary constraint in (9f) to a box constraint and introduce a penalty function to ensure convergence to a binary solution. We then employ AO to decouple the problem into two sub-problems. The non-convexity of the two sub-problems is addressed using convex approximations, mathematical transformations, the S-procedure, and general sign-definiteness. In the following, we present Lemma 1 and Lemma 2 which will be highly instrumental in solving the formulated problem.

Lemma 1. *(The S-Lemma [68], [69]): Considering the following quadratic function of variable x*

$$f_t(\mathbf{x}) = \mathbf{x}^H \mathbf{A}_t \mathbf{x} + 2\,\mathrm{Re}\left\{\mathbf{a}_t^H \mathbf{x}\right\} + c_t. \tag{11}$$

Here $\mathbf{A}_t \in \mathbb{C}^{N\times N}$ is a Hermitian matrix, $\mathbf{a}_t \in \mathbb{C}^{N\times 1}$ and $c_t \in \mathbb{R}$. The implication $f_1(\mathbf{x}) \leq 0 \Rightarrow f_2(\mathbf{x}) \leq 0$ holds if and only if there exists a $\delta \geq 0$ such that

$$\delta \begin{bmatrix} \mathbf{A}_1 & \mathbf{a}_1 \\ \mathbf{a}_1^H & c_1 \end{bmatrix} - \begin{bmatrix} \mathbf{A}_2 & \mathbf{a}_2 \\ \mathbf{a}_2^H & c_2 \end{bmatrix} \succeq \mathbf{0}, \tag{12}$$

Note that S-Lemma is also referred to as the S-procedure in this work.

Lemma 2. *(The Sign-Definiteness Lemma [32], [70]): Given a set of Hermitian matrices $\mathbf{A}, \{\mathbf{Q}_t, \mathbf{F}_t\}_{t=1}^Z$, the linear matrix inequality (LMI) shown below satisfies*

$$\mathbf{A} \succeq \sum_{t=1}^{Z} \left(\mathbf{Q}_i^{\mathrm{H}} \mathbf{X}_t \mathbf{F}_t + \mathbf{F}_t^{\mathrm{H}} \mathbf{X}_t^{\mathrm{H}} \mathbf{Q}_t\right), \forall t, \|\mathbf{X}_t\|_F \leq \zeta_t, \tag{13}$$

if and only if there exist real numbers $\forall t, \mu_t \geq 0$ such that

$$\begin{bmatrix} \mathbf{A} - \sum_{t=1}^{Z} \mu_t \mathbf{F}_t^{\mathrm{H}} \mathbf{F}_t & -\zeta_1 \mathbf{Q}_1^{\mathrm{H}} & \cdots & -\zeta_Z \mathbf{Q}_Z^{\mathrm{H}} \\ -\zeta_1 \mathbf{Q}_1 & \mu_1 \mathbf{I} & \cdots & \mathbf{0} \\ \vdots & \vdots & \ddots & \vdots \\ -\zeta_Z \mathbf{Q}_Z & \mathbf{0} & \cdots & \mu_Z \mathbf{I} \end{bmatrix} \succeq \mathbf{0}. \tag{14}$$

In the next section, we detail the steps to solving the formulated problem.

IV. Proposed Solution

A. Problem Reformulation and Binary Variable Relaxation

In this section, we detail the proposed solution to solve the formulated problem in (9). Firstly, we introduce an auxiliary variable to handle the non-smooth objective function into a smooth one as follows:

$$z = \min_{\ell \in \mathcal{L}} \boldsymbol{\psi}_\ell^T \boldsymbol{a}. \tag{15}$$

Accordingly, problem (9) can be reformulated as follows:

$$\begin{aligned}
\underset{\boldsymbol{\phi},\mathbf{W},\boldsymbol{a},z}{\text{maximize}}\ & z && \text{(16a)}\\
\text{s. t.}\quad & \gamma_k(\mathbf{W},\boldsymbol{\phi}) \geq a_k \Gamma_k^{\text{th}}, \forall \|\boldsymbol{\Psi}_k\| \leq \zeta_k, \forall k \in \mathcal{K}, && \text{(16b)}\\
& \sum_{k\in\mathcal{K}} \|\mathbf{w}_k\|^2 \leq P^{\max}, && \text{(16c)}\\
& \|\mathbf{w}_k\|^2 \leq a_k P^{\max}, \forall k \in \mathcal{K}, && \text{(16d)}\\
& |\boldsymbol{\phi}_{n,\ell}| = 1,\ \forall n \in \mathcal{N}, \forall \ell \in \mathcal{L}, && \text{(16e)}\\
& a_k \in \{0,1\},\ \forall k \in \mathcal{K}, && \text{(16f)}\\
& \boldsymbol{\psi}_\ell^T \boldsymbol{a} \geq z,\ \forall \ell \in \mathcal{L}. && \text{(16g)}
\end{aligned}$$

The first step in tackling problem (16) is to relax the binary variables in constraint (16f) to a continuous variable. Following this step, we obtain the following relaxed problem,

$$\begin{aligned}
\underset{\boldsymbol{\phi},\mathbf{W},\boldsymbol{a},z}{\text{maximize}}\ & z && \text{(17a)}\\
\text{s. t.}\quad & 0 \leq a_k \leq 1, \forall k \in \mathcal{K}, && \text{(17b)}\\
& a_k - a_k^2 \leq 0, \forall k \in \mathcal{K}, && \text{(17c)}\\
& \text{(16b), (16c), (16d), (16e), (16g).}
\end{aligned}$$

It is important to note that constraint (16f) has been substituted by (17b) and (17c). Here, (17b) is a box constraint and (17c) is an additional constraint to ensure that a_k is binary at convergence. To convexify the additional constraint (17c), we approximate the non-convex parts to obtain a lower-bound approximation using the first-order Taylor approximation. In addition, following [71, Preposition 2], we solve the problem by choosing a penalty parameter $\mu > 0$. Accordingly, we present a penalty function as follows: $\mathcal{Q}(\boldsymbol{a}) = \mu\Big(\sum_{k\in\mathcal{K}} a_k^2 - \sum_{k\in\mathcal{K}} a_k\Big)$. Note that the effect of this penalty function is modeled in the objective function. Next, after approximating $\sum_{k\in\mathcal{K}} a_k^2$, by applying the first order Taylor approximation of $\mathcal{Q}(\boldsymbol{a})$ for a_k around a feasible point a_k^ι, we obtain $\mathcal{Q}^{\text{t}}(\boldsymbol{a}) = \mu\Big[\sum_{k\in\mathcal{K}} \big(2a_k^\iota a_k - (a_k^\iota)^2\big) - \sum_{k\in\mathcal{K}} a_k\Big]$. Now, by choosing an appropriate penalty parameter, problem (17) can be tackled by solving the following problem with updating $\mathcal{Q}^{\text{t}}(\boldsymbol{a})$ iteratively. Accordingly, we reformulate the overall problem as follows:

$$\begin{aligned}
\underset{\boldsymbol{\phi},\mathbf{W},\boldsymbol{a},z}{\text{minimize}}\ & -z - \mathcal{Q}^{\text{t}}(\boldsymbol{a}) && \text{(18a)}\\
\text{s. t.}\quad & \gamma_k(\mathbf{W},\boldsymbol{\phi}) \geq a_k \Gamma_k^{\text{th}}, \forall \|\boldsymbol{\Psi}_k\| \leq \zeta_k, \forall k \in \mathcal{K}, && \text{(18b)}\\
& \sum_{k\in\mathcal{K}} \|\mathbf{w}_k\|^2 \leq P^{\max}, && \text{(18c)}\\
& \|\mathbf{w}_k\|^2 \leq a_k P^{\max}, \forall k \in \mathcal{K}, && \text{(18d)}\\
& |\boldsymbol{\phi}_{n,\ell}| = 1,\ \forall n \in \mathcal{N},\ \forall \ell \in \mathcal{L}, && \text{(18e)}\\
& 0 \leq a_k \leq 1,\ \forall k \in \mathcal{K}, && \text{(18f)}\\
& \psi_\ell \boldsymbol{a} \geq z,\ \forall \ell \in \mathcal{L}. && \text{(18g)}
\end{aligned}$$

Even after relaxing the binary variable, problem (18) remains non-convex due to the coupled variables in constraint (18b). Additionally, the channel estimation error in (18b) further complicates the direct solution of the problem. To address this complexity, we employ an AO approach to decouple the BS precoding and RIS phase shift variables, solving them alternately. Convex approximations are employed to manage the non-convexity, while the S-procedure and general sign-definiteness techniques, as detailed in Lemma 1 and Lemma 2, are utilized to handle channel uncertainty. The following sections outline the steps to solve the two sub-problems.

B. Base-Station Precoding Design

For a given $\boldsymbol{\phi}$, we optimize the precoding design to maximize the minimum number of well-served users in proximity to each RIS subject to the total available power at the BS and the worst-case SINR constraints. The resulting problem is formulated as follows

$$\begin{aligned}
\underset{\mathbf{W},\boldsymbol{a},z}{\text{minimize}}\ & -z - \mathcal{Q}^{\text{t}}(\boldsymbol{a}) && \text{(19a)}\\
\text{s. t.}\quad & \gamma_k(\mathbf{W},\boldsymbol{\phi}) \geq a_k \Gamma_k^{\text{th}}, \forall \|\boldsymbol{\Psi}_k\| \leq \zeta_k, \forall k \in \mathcal{K}, && \text{(19b)}\\
& \sum_{k\in\mathcal{K}} \|\mathbf{w}_k\|^2 \leq P^{\max}, && \text{(19c)}\\
& \|\mathbf{w}_k\|^2 \leq a_k P^{\max}, \forall k \in \mathcal{K}, && \text{(19d)}\\
& 0 \leq a_k \leq 1,\ \forall k \in \mathcal{K}, && \text{(19e)}\\
& \psi_\ell \boldsymbol{a} \geq z,\ \forall \ell \in \mathcal{L}. && \text{(19f)}
\end{aligned}$$

The main challenge in solving problem (19) is the non-convexity of the semi-infinite constraints in (19b). Additionally, the solution should be feasible $\forall \|\boldsymbol{\Psi}_k\| \leq \zeta_k$. To address these challenges, consequently, we focus on convexifying the non-convex parts of the problem by employing convex approximation techniques studied in [35].

In particular, following *Lemma* 1 and *Lemma* 2, we tackle the multiple complex valued uncertainties. First, we introduce a new auxiliary variable representing the soft interference threshold for user k as $\eta_k = \sum_{i\in\mathcal{K}/\{k\}} \big|(\mathbf{h}_k^H + \sum_{\ell\in\mathcal{L}} \psi_{k,\ell} \boldsymbol{\phi}_\ell^H \mathbf{H}_{\ell,k})\mathbf{w}_i\big|^2 + \sigma_k^2, (\forall k \in \mathcal{K})$. Accordingly, we reformulate constraint (19b) as follows

$$\frac{\big|(\mathbf{h}_k^H + \sum_{\ell\in\mathcal{L}} \psi_{k,\ell} \boldsymbol{\phi}_\ell^H \mathbf{H}_{\ell,k})\mathbf{w}_k\big|^2}{\eta_k} \geq a_k \Gamma_k^{\text{th}}, \quad \forall \|\boldsymbol{\Psi}_k\| \leq \zeta_k, \forall k \in \mathcal{K}, \forall \ell \in \mathcal{L}, \tag{20}$$

and

$$\sum_{i\in\mathcal{K}/\{k\}} \big|(\mathbf{h}_k^H + \sum_{\ell\in\mathcal{L}} \psi_{k,\ell} \boldsymbol{\phi}_\ell^H \mathbf{H}_{\ell,k})\mathbf{w}_i\big|^2 + \sigma_k^2 \leq \eta_k, \quad \forall \|\boldsymbol{\Psi}_k\| \leq \zeta_k, \forall k \in \mathcal{K}, \forall \ell \in \mathcal{L}. \tag{21}$$

Herein, (20) is termed the worst-case useful signal power constraint and (21) is the worst-case interference power constraint, respectively. Note that the function $\frac{\big|(\mathbf{h}_k^H + \sum_{\ell\in\mathcal{L}} \psi_{k,\ell} \boldsymbol{\phi}_\ell^H \mathbf{H}_{\ell,k})\mathbf{w}_k\big|^2}{\eta_k}$ in (20) is in quadratic-over-linear form which can be easily approximated by obtaining its lower

bound using first-order Taylor series approximation. Based on this approximation, an iterative approach is proposed to solve problem (19). Specifically, we analyze the lower bound of the left-hand side (L.H.S) of (20) in the following proposition.

Proposition 1. *For any feasible* $\mathbf{w}_k^{(\iota)}$ *and* $\eta_k^{(\iota)}$*, one can define an effective lower bound for the L.H.S of* (20) *as follows,*

$$\frac{\left|\left(\mathbf{h}_k^H+\sum\limits_{\ell\in\mathcal{L}}\psi_{k,\ell}\boldsymbol{\phi}_\ell^H\mathbf{H}_{\ell,k}\right)\mathbf{w}_k\right|^2}{\eta_k}\geq\mathbf{v}_k^H\boldsymbol{T}_k\mathbf{v}_k+2\Re\{\boldsymbol{t}_k^T\mathbf{v}_k\}+t_k, \tag{22}$$

where $\mathbf{v}_k=\mathrm{vec}\left(\sum_{\ell\in\mathcal{L}}\psi_{\ell,k}\boldsymbol{\Psi}_{\ell,k}^*\right)$ *while* $\boldsymbol{T}_k$*,* $\boldsymbol{t}_k$*, and* t_k *are given as*

$$t_k=2\Re\{\mathbf{q}_k^H\mathbf{w}_k^{(\iota)}\mathbf{w}_k^H\mathbf{q}_k\}(\eta_k^\iota)^{-1}-\mathbf{q}_k^H\mathbf{w}^{(\iota)}\mathbf{w}_k^{(\iota),H}\mathbf{q}_k\eta_k(\eta_k^\iota)^{-2}, \tag{23}$$

$$\begin{aligned}\boldsymbol{t}_k=&\mathrm{vec}\big(\mathbf{Q}_k\mathbf{w}_k^{(\iota)}\mathbf{w}_k^H\big)(\eta_k^\iota)^{-1}+\mathrm{vec}\big(\mathbf{Q}_k\mathbf{w}_k\mathbf{w}_k^{(\iota),H}\big)(\eta_k^\iota)^{-1}\\&-\mathrm{vec}\big(\mathbf{Q}_k\mathbf{w}_k^{(\iota)}\mathbf{w}_k^{(\iota),H}\big)\eta_k(\eta_k^\iota)^{-2},\end{aligned} \tag{24}$$

$$\begin{aligned}\boldsymbol{T}_k=&\big(\mathbf{w}_k\mathbf{w}_k^{(\iota),H}\otimes\boldsymbol{\Phi}_k\big)(\eta_k^\iota)^{-1}+\big(\mathbf{w}_k^{(\iota)}\mathbf{w}_k^H\otimes\boldsymbol{\Phi}_k\big)(\eta_k^\iota)^{-1}\\&-\big(\mathbf{w}^{(\iota)}\mathbf{w}_k^{(\iota),H}\otimes\boldsymbol{\Phi}_k\big)\eta_k(\eta_k^\iota)^{-2},\end{aligned} \tag{25}$$

in which $\mathbf{q}_k=\mathbf{h}_k+\sum_{\ell\in\mathcal{L}}\psi_{\ell,k}\hat{\mathbf{H}}_{\ell,k}^H\boldsymbol{\phi}_\ell$*,* $\mathbf{Q}_k=\sum_{\ell\in\mathcal{L}}\psi_{\ell,k}\boldsymbol{\phi}_\ell\mathbf{q}_k^H$*, and* $\boldsymbol{\Phi}_k=\sum_{\ell\in\mathcal{L}}\psi_{\ell,k}\boldsymbol{\phi}_\ell^*\boldsymbol{\phi}_\ell^T$*.*

Proof: The proof can be obtained by following the procedure given in [35] which is summarized in the Appendix. ∎

Thanks to Proposition 1, by substituting the corresponding lower bound into (20), we obtain the following expression

$$\mathbf{v}_k^H\boldsymbol{T}_k\mathbf{v}_k+2\Re\{\boldsymbol{t}_k^T\mathbf{v}_k\}+t_k\geq a_k\Gamma_k^{\mathrm{th}},\forall\|\boldsymbol{\Psi}_k\|\leq\zeta_k,\forall k,\forall\ell. \tag{26}$$

To tackle the channel uncertainty in (26), we resort to the S-procedure in *Lemma* 1. First, we define a slack variable $\boldsymbol{\delta}=[\delta_k,\cdots,\delta_k]^T\geq 0$. Then, by applying the S-Lemma in Lemma 1, we transform (26) into the following equivalent linear matrix inequalities (LMIs)

$$\begin{bmatrix}\delta\boldsymbol{I}_{\mathrm{NxM}}+\boldsymbol{T}_k & \boldsymbol{t}_k^H\\ \boldsymbol{t}_k & t_k-a_k\Gamma_k^{\mathrm{th}}-\delta_k\zeta_k^2\end{bmatrix}\succeq 0,\forall k. \tag{27}$$

Next, we can apply Schur's complement to handle the worst-case interference power constraint in (21). In this case, we let $\mathbf{W}_{-k}=[\mathbf{w}_1,\cdots,\mathbf{w}_{k-1},\mathbf{w}_{k+1},\cdots,\mathbf{w}_K]\in\mathbb{C}^{M\times(K-1)}$. Accordingly, we recast interference-plus-noises (INs) in (21) into the following matrix inequalities [72].

$$\begin{aligned}&\begin{bmatrix}\eta_k-\sigma_k^2 & \mathbf{m}_k^H\\ \mathbf{m}_k & \boldsymbol{I}_{(K-1)}\end{bmatrix}\\&\succeq-\begin{bmatrix}\mathbf{0}_{1\times M}\\ \mathbf{W}_{-k}^H\end{bmatrix}\sum_{\ell\in\mathcal{L}}\left(\psi_{\ell,k}\boldsymbol{\Psi}_{\ell,k}^H\begin{bmatrix}\mathbf{0}_{N\times 1} & \big[\boldsymbol{\phi}_\ell\big]_{1\times(K-1)}\end{bmatrix}\right)\\&-\sum_{\ell\in\mathcal{L}}\left(\begin{bmatrix}\big[\boldsymbol{\phi}_\ell^H\big]_{(K-1)\times 1}\\ \mathbf{0}_{1\times N}\end{bmatrix}\psi_{\ell,k}\boldsymbol{\Psi}_{\ell,k}\right)\begin{bmatrix}\mathbf{0}_{M\times 1} & \mathbf{W}_{-k}\end{bmatrix},\forall k,\end{aligned} \tag{28}$$

where, $\mathbf{m}_k=\left(\left(\mathbf{h}_k^H+\sum_{\ell\in\mathcal{L}}\psi_{\ell,k}\boldsymbol{\phi}_\ell^H\hat{\mathbf{H}}_{\ell,k}\right)\mathbf{W}_{-k}\right)^H\in\mathbb{C}^{(K-1)\times 1}$. Next we define the slack variable $\boldsymbol{\upsilon}=[\upsilon_1\cdots\upsilon_k]^T\geq 0$. Then, employing the general sign definiteness in *Lemma* 2 yields the following equivalent LMIs

$$\begin{bmatrix}\eta_k-\sigma_k^2-\upsilon_kN & \mathbf{m}_k^H & \mathbf{0}_{1\times M}\\ \mathbf{m}_k & \boldsymbol{I}_{K-1} & \zeta_k\mathbf{W}_{-k}^H\\ \mathbf{0}_{M\times 1} & \zeta_k\mathbf{W}_{-k} & \upsilon_k\boldsymbol{I}_M\end{bmatrix}\succeq 0,\forall k. \tag{29}$$

Substituting the linearized constraints, accordingly, at iteration $\iota+1$, problem (19) can be re-stated as

$$\begin{aligned}\mathscr{P}:\quad&\underset{\mathbf{W},\boldsymbol{a},\boldsymbol{\delta},\boldsymbol{\eta},z,\boldsymbol{\upsilon}}{\text{minimize}}\ f_{\mathbf{W}}^{(\iota)}(z)\triangleq-z-\mathcal{Q}^{\mathrm{t}}(\boldsymbol{a}) && \text{(30a)}\\&\text{s. t.}\quad(27),(29),(19\text{c})-(19\text{f}) && \text{(30b)}\\&\qquad\boldsymbol{\delta}\geq 0,\boldsymbol{\eta}\geq 0,\boldsymbol{\upsilon}\geq 0 && \text{(30c)}\end{aligned}$$

where $\boldsymbol{\eta}$ stands for $[\eta_1,\cdots,\eta_k]^T$. Problem (30) is convex and can be solved using convex optimization tools e.g. CVX [73].

C. Passive RIS-Beamforming Design

For a given precoding matrix $\mathbf{W}$, we aim to optimize the RIS phase shifts by addressing the following problem,

$$\begin{aligned}&\underset{\boldsymbol{\phi},\mathbf{W},\boldsymbol{a},z}{\text{minimize}}\ -z-\mathcal{Q}^{\mathrm{t}}(\boldsymbol{a}), && \text{(31a)}\\&\text{s. t.}\quad\gamma_k(\mathbf{W},\boldsymbol{\phi})\geq a_k\Gamma_k^{\mathrm{th}},\forall\|\boldsymbol{\Psi}_k\|\leq\zeta_k,\forall k\in\mathcal{K}, && \text{(31b)}\\&\qquad|\boldsymbol{\phi}_{n,\ell}|=1,\ \forall n\in\mathcal{N},\forall\ell\in\mathcal{L}, && \text{(31c)}\\&\qquad 0\leq a_k\leq 1,\ \forall k\in\mathcal{K}, && \text{(31d)}\\&\qquad\psi_\ell\boldsymbol{a}\geq z,\ \forall\ell\in\mathcal{L}. && \text{(31e)}\end{aligned}$$

Following a similar procedure in the previous subsection, we first tackle the nonconvexity of constraint (31b). Specifically, we reformulate constraint (31b) as (20) and (21) to facilitate solving problem (31). To convexify the L.H.S of (20), we derive its lower bound in the following proposition.

Proposition 2. *For any feasible* $\boldsymbol{\phi}_k^{(\iota)}$ *and* $\eta_k^{(\iota)}$*, we can define the L.H.S of* (20) *as follows*

$$\frac{\left|\left(\mathbf{h}_k^H+\sum\limits_{\ell\in\mathcal{L}}\psi_{k,\ell}\boldsymbol{\phi}_\ell^H\mathbf{H}_{\ell,k}\right)\mathbf{w}_k\right|^2}{\eta_k}\geq\mathbf{v}_k^H\tilde{\boldsymbol{T}}_k\mathbf{v}_k+2\Re\{\tilde{\boldsymbol{t}}_k^T\mathbf{v}_k\}+\tilde{t}_k, \tag{32}$$

where $\mathbf{v}_k=\mathrm{vec}\left(\sum_{\ell\in\mathcal{L}}\psi_{\ell,k}\boldsymbol{\Psi}_{\ell,k}^*\right)$ *while* $\tilde{\boldsymbol{T}}_k$*,* $\tilde{\boldsymbol{t}}_k$*, and* $\tilde{t}_k$ *are given as*

$$\tilde{t}_k=2\Re\{\tilde{\mathbf{q}}_k^{(\iota),H}\mathbf{w}_k\mathbf{w}_k^H\tilde{\mathbf{q}}_k\}(\eta_k^{(\iota)})^{-1}-\tilde{\mathbf{q}}_k^{(\iota),H}\mathbf{w}\mathbf{w}_k^H\tilde{\mathbf{q}}_k^\iota\eta_k(\eta_k^\iota)^{-2}, \tag{33}$$

$$\begin{aligned}\tilde{\boldsymbol{t}}_k=&\mathrm{vec}\big(\tilde{\mathbf{Q}}_{1,k}\mathbf{w}\mathbf{w}_k^H\big)(\eta_k^\iota)^{-1}+\mathrm{vec}\big(\mathbf{Q}_{2,k}\mathbf{w}_k\mathbf{w}_k\big)(\eta_k^\iota)^{-1}\\&-\mathrm{vec}\big(\mathbf{Q}_{3,k}\mathbf{w}_k^{(\iota)}\mathbf{w}_k^{(\iota),H}\big)\eta_k(\eta_k^\iota)^{-2},\end{aligned} \tag{34}$$

$$\begin{aligned}\tilde{\boldsymbol{T}}_k=&\big(\mathbf{w}_k\mathbf{w}_k^{(\iota),H}\otimes\tilde{\boldsymbol{\Phi}}_{1,k}\big)(\eta_k^\iota)^{-1}+\big(\mathbf{w}_k^{(\iota)}\mathbf{w}_k^H\otimes\tilde{\boldsymbol{\Phi}}_{2,k}\big)(\eta_k^\iota)^{-1}\\&-\big(\mathbf{w}^{(\iota)}\mathbf{w}_k^{(\iota),H}\otimes\tilde{\boldsymbol{\Phi}}_{3,k}\big)\eta_k(\eta_k^\iota)^{-2},\end{aligned} \tag{35}$$

in which $\tilde{\mathbf{q}}_k^{(\iota),H}=\mathbf{h}_k^H+\sum_{\ell\in\mathcal{L}}\psi_{\ell,k}\boldsymbol{\phi}_\ell^{(\iota),H}\hat{\mathbf{H}}_{\ell,k}$*,* $\tilde{\mathbf{q}}_k=\mathbf{h}_k+\sum_{\ell\in\mathcal{L}}\psi_{\ell,k}\hat{\mathbf{H}}_{\ell,k}^H\boldsymbol{\phi}_\ell$*,* $\tilde{\mathbf{q}}_k^{(\iota)}=\mathbf{h}_k^H+\sum_{\ell\in\mathcal{L}}\psi_{\ell,k}\boldsymbol{\phi}_\ell^{(\iota),H}\hat{\mathbf{H}}_{\ell,k}$*,* $\tilde{\mathbf{Q}}_{1,k}=\sum_{\ell\in\mathcal{L}}\psi_{\ell,k}\boldsymbol{\phi}_\ell\tilde{\mathbf{q}}_k^{(\iota),H}$*,* $\tilde{\mathbf{Q}}_{2,k}=\sum_{\ell\in\mathcal{L}}\psi_{\ell,k}\boldsymbol{\phi}_\ell^{(\iota)}\tilde{\mathbf{q}}_k$*,* $\tilde{\mathbf{Q}}_{3,k}=\sum_{\ell\in\mathcal{L}}\psi_{\ell,k}\boldsymbol{\phi}_\ell^{(\iota)}\tilde{\mathbf{q}}_k^{(\iota),H}$*,*

Algorithm 1 PROPOSED ALTERNATING OPTIMIZATION ALGORITHM

Initialization: Set $\iota = 1$ and initialize feasible points for $(\mathbf{W}^{(0)}, \boldsymbol{\phi}^{(0)}, \mathbf{a}^{(0)}, \boldsymbol{\eta}^{(0)})$.
1: **repeat**
2: Solve (30) for given $\boldsymbol{\phi}^{(\iota)}$ to obtain the optimal solutions $(\mathbf{a}^*, \mathbf{W}^*, \boldsymbol{\eta}^*)$ and update $(\mathbf{a}^{(\iota+1)}, \mathbf{W}^{(\iota+1)}, \boldsymbol{\eta}^{(\iota+1)}) := ((\mathbf{a}^*, \mathbf{W}^*, \boldsymbol{\eta}^*)$;
3: Solve (39) for given $(\mathbf{W}^{(\iota+1)})$ to obtain the optimal solutions $(\boldsymbol{\phi}^*, \boldsymbol{\eta}^*)$ and update $(\mathbf{a}^*, \boldsymbol{\phi}^{(\iota+1)}, \boldsymbol{\eta}^{(\iota+1)}) := (\mathbf{a}^*, \boldsymbol{\phi}^*, \boldsymbol{\eta}^*)$;
4: Set $\iota = \iota + 1$;
5: **until** The fractional decrease in objective value is less than α.
6: **Output:** $(\mathbf{W}^*, \boldsymbol{\phi}^*, \mathbf{a}^*)$.

$\tilde{\boldsymbol{\Phi}}_{1,k} = \sum_{\ell\in\mathcal{L}} \psi_{\ell,k}\boldsymbol{\phi}_\ell^*\boldsymbol{\phi}_\ell^{(\iota),T}$, $\tilde{\boldsymbol{\Phi}}_{2,k} = \sum_{\ell\in\mathcal{L}} \psi_{\ell,k}\boldsymbol{\phi}_\ell^{(\iota),*}\boldsymbol{\phi}_\ell^{T}$, *and* $\tilde{\boldsymbol{\Phi}}_{3,k} = \sum_{\ell\in\mathcal{L}} \psi_{\ell,k}\boldsymbol{\phi}_\ell^{(\iota),*}\boldsymbol{\phi}_\ell^{(\iota),T}$.

Proof: The proof is summarized in the Appendix, following the procedure given in [35]. ∎

Substituting (32) into the worst-case useful signal power, we get the following

$$\mathbf{v}_k^H\tilde{\boldsymbol{T}}_k\mathbf{v}_k + 2\Re\{\tilde{\boldsymbol{t}}_k^T\mathbf{v}_k\} + \tilde{t}_k \geq a_k\Gamma_k^{\text{th}}, \forall \|\boldsymbol{\Psi}_k\| \leq \zeta_k, \forall k, \forall \ell. \quad (36)$$

Next, we employ the S-procedure (S-Lemma) in *Lemma* 1 to tackle the channel uncertainty in (36). Let $\tilde{\boldsymbol{\delta}} = [\tilde{\delta}_k, \cdots, \tilde{\delta}_k]^T \geq 0$ be a slack variable and let $\tilde{\boldsymbol{\upsilon}} = [\tilde{\upsilon}_1 \cdots \tilde{\upsilon}_k]^T \geq 0$. Applying the S-Lemma, we transform (36) into the equivalent LMIs as follows

$$\begin{bmatrix} \tilde{\delta}_k\boldsymbol{I}_{\text{LN}_1\text{xM}} + \tilde{\boldsymbol{T}}_k & \tilde{\boldsymbol{t}}_k^H \\ \tilde{\boldsymbol{t}}_k & \tilde{t}_k - a_k\Gamma_k^{\text{th}} - \tilde{\delta}_k\zeta_k^2 \end{bmatrix} \succeq 0, \forall k, \quad (37)$$

In addition, we recast INs into matrix inequalities. Removing the unrelated part to $\boldsymbol{\phi}$ from the LMIs in (29), one yields

$$\begin{bmatrix} \eta_k - \sigma_k^2 - \tilde{\upsilon}_k N & \mathbf{m}_k^H \\ \mathbf{m}_k & \boldsymbol{I}_{K-1} \end{bmatrix} \succeq 0, \forall k. \quad (38)$$

Accordingly, at iteration $\iota+1$, we optimize the RIS phase shift design as follows

$$\underset{\boldsymbol{\phi},\boldsymbol{a},\boldsymbol{\eta},z,\tilde{\boldsymbol{\upsilon}},\tilde{\boldsymbol{\delta}}}{\text{minimize}} \; f_{\boldsymbol{\phi}}^{(\iota)}(z) \triangleq -z - \mathcal{Q}^{\text{t}}(\boldsymbol{a}) \quad (39a)$$

$$\text{s. t.} \quad (37), (38), (31\text{c}), (31\text{d}), (31\text{e}) \quad (39b)$$

$$\tilde{\boldsymbol{\delta}} \geq 0, \boldsymbol{\eta} \geq 0, \tilde{\boldsymbol{\upsilon}} \geq 0. \quad (39c)$$

Here $\boldsymbol{\eta}$ stands for $[\eta_1, \cdots, \eta_k]^T$. As can be observed, problem 39 is non-convex due to the unit modulus constraint in (31c). To avoid increasing the complexity of problem (39), we relax the non-convex constraint (31c) to a convex inequality constraint, followed by normalization to ensure equality at convergence. The phase shift design problem can also be solved using the penalty convex-concave procedure (CCP) method, as detailed in [35]. Consequently, the reformulated problem becomes convex and can be solved using standard convex optimization tools such as CVX [73].

D. Joint Robust BS-Precoding and RIS-Beamforming Design

The overall joint robust BS-precoding and RIS-BF design for solving problem (9) is summarized in Algorithm 1. In particular, the solution process initializes by selecting a feasible point for $(\mathbf{W}^{(0)}, \boldsymbol{\phi}^{(0)}, \mathbf{a}^{(0)}, \boldsymbol{\eta}^{(0)})$. Then, the algorithm tends to optimize $\{\mathbf{a}, \mathbf{W}, \boldsymbol{\eta}\}$ for given $\boldsymbol{\phi}$ and $\{\mathbf{a}, \boldsymbol{\phi}, \boldsymbol{\eta}\}$ for given $\mathbf{W}$, alternatively in each following iteration. This can be done by solving (30) and (39) for given $\boldsymbol{\phi}$ and $\mathbf{W}$, respectively. The iterative procedure continues until the fractional decrease in the value of the objective function for the overall problem is less than a predefined threshold $\alpha = 10^{-3}$.

1) Convergence Analysis: The convergence of Algorithm 1 is discussed in the following proposition.

Proposition 3. *Algorithm 1 converges to a fixed point after a finite number of iterations.*

Proof: As proved in [74], Algorithm 1 generates a sequence of $\{\mathbf{W}^{(*)}, \boldsymbol{\phi}^{(*)}, \boldsymbol{a}^{(*)}, \boldsymbol{\eta}^{(*)}\}$'s which corresponds to non-decreasing objective values of problem (9) as well as the cost function. As a result, the stationary point of the original problem is obtained after a sufficient number of iterations. ∎

Additionally, the simulation results in the following section numerically verify the convergence analysis.

2) Complexity Analysis: The complexity of implementing Algorithm 1 mainly depends on solving (30) and (39) in each iteration. As analyzed in [75, Chapter 6], the worst-case complexity of solving problem (30) using the interior point method is given by

$$X_{(30)} = \mathcal{O}\big(\sqrt{2KL + 6K + L}(MK + 4K + 1)^3\big). \quad (40)$$

While the worst-case complexity of solving problem (39) using the interior point method is given by

$$X_{(39)} = \mathcal{O}\big(\sqrt{2KL + NL + 4K + L}(NL + 4K + 1)^3\big). \quad (41)$$

Let J^{iter} be the iteration number required for Algorithm 1 converging. This algorithm's complexity can be estimated as

$$X^{\text{total}} = J^{\text{iter}}\left(X_{(30)} + X_{(39)}\right). \quad (42)$$

3) Selection of the penalty parameter μ: Selecting an appropriate penalty parameter is critical to ensure the overall system performance of Algorithm 1. It is observed that choosing a large value for μ may accelerate the convergence of Algorithm 1 and lead to an exact binary solution. However, this can also result in significant performance degradation due to improper convergence. In our simulations, we found that setting the penalty parameter to a sufficiently small value, $\mu = 0.002$ guarantees the convergence of Algorithm 1 while maintaining the best performance [50].

4) Feasible points initialization: The initial feasible points for the first iteration of the proposed algorithm are generated as follows. First, we randomly generate $\mathbf{a}^{(0)}$ and $\boldsymbol{\phi}^{(0)}$ to satisfy constraints $(22f)$ and $(22e)$, respectively. This ensures that the initial points comply with the respective constraints. For simplicity, the feasible point of the precoder $\mathbf{W}^{(0)}$ is randomly generated with equal power allocation. Next, we generate the soft interference threshold $\boldsymbol{\eta}^{(0)}$ by setting $\eta_k^{(0)} = \sum_{i\in\mathcal{K}/k}\left|(\mathbf{h}_k^H + \sum_{\ell\in\mathcal{L}}\psi_{k,\ell}\boldsymbol{\phi}_\ell^{(0),H}\mathbf{H}_{\ell,k})\mathbf{w}_i^{(0)}\right|^2 + \sigma_k^2, \forall k \in \mathcal{K}$.

V. NUMERICAL RESULTS

This section provides a detailed discussion of the presented numerical results to evaluate the performance of the proposed

TABLE II: SIMULATION PARAMETERS

Parameter	Value
Carrier frequency (f_c)	2.4 GHz
BS transmit power (P^{max})	38 dBm
Noise power	-90 dBm
Number of RIS (L)	3
pathloss exponent BS-RIS (α_{br})	2.7
pathloss exponent RIS-user (α_{ru})	2.3
Antenna and element spacing	0.5λ
Rician factor (ξ)	3 dB
Penalty parameter (μ)	0.002

robust max-min fairness design for a multi-RIS-aided system. We consider a 3-D system model, where the BS is deployed at the origin with the height of 10 m i.e at position $(0, 0, 10)$. The users are randomly distributed with uniform probability density as illustrated in Fig. 1 into three different groups or locations representing the different hotspot areas. In hotspot 1, 2 and 3, users are distributed between 10 and 30 m in the y-axis, -10 and -30 m in the y-axis and 50 and 70 m in the x-axis, respectively. Note that the height of the users is fixed at 1.5 m. It is worth mentioning that the RISs and the users in their respective hotspot areas are not co-located. However, the RISs are deployed close to their respective coverage area (hotspot) for better performance. Accordingly, an RIS is deployed close to each hotspot area as follows: $(-5, 20, 3)$, $(-5, -20, 3)$, and $(60, -5, 3)$. In this case, this follows the user-side RIS deployment. For better performance, the height of the RIS is set at 3 m which is close to the height of the users in the hotspot areas [26]. It is important to note that, for all our simulations, the direct link from the BS to the users is assumed to be unavailable i.e. $\mathbf{h}_k = \mathbf{0}_{M\times 1}, \forall k \in \mathcal{K}$. In this case, the RISs are deployed as alternative paths to serve users in the hotspot areas. Unless otherwise stated, the other setting parameters can be found in Table II.

Regarding the channel model, we employ a Rician channel model for all the channels. In particular, the RIS ℓ to user k channel $\mathbf{g}_{\ell,k}$ can be written as $\mathbf{g}_{\ell,k} = \sqrt{\frac{\xi}{1+\xi}}\mathbf{g}_{\ell,k}^{\text{LOS}} + \sqrt{\frac{1}{1+\xi}}\mathbf{g}_{\ell,k}^{\text{NLOS}}$, where $\mathbf{g}_{\ell,k}^{\text{LOS}}$ and $\mathbf{g}_{\ell,k}^{\text{NLOS}}$ denote the LOS and NLOS components, respectively. In this case, ξ denotes the considered Rician factor. In addition, the distance-dependent path loss is modeled as follows $PL = -30 - 10\alpha \log_{10}(d)$ dB where d is the link distance between two nodes and α is the path loss exponent [32]. Note that the constant -30 dB is the path loss at reference distance 1 m. In addition, the error bound of the CSI for the cascaded BS-RIS-user k channel is defined as $\zeta_k = \varrho\|\hat{\mathbf{H}}_k\|$. In this case, $\varrho \in [0, 1]$ is the measure of the relative amount of uncertainty. The simulation results in this work are averaged over 10^3 channel realizations. To evaluate the performance of the proposed design, we compare the proposed scheme with the following three baseline schemes:

- Max-sum: One aims to maximize the total number of well-served users assisted by all the RISs for all possible channel error realizations without considering fairness. This design was considered in [27] assuming the availability of perfect CSI for a system with a single RIS. Accordingly, for a fair comparison with the robust max-min fairness design in a multi-RIS-aided network, we designed the robust max-sum as a baseline scheme for the considered system model.
- Max-sum random phase: One aims to optimize the total well-served user number assisted by all RISs without optimizing the RIS phase shifts. In this case, the RISs are deployed in different hotspot areas as random scatterers.
- Max-min random phase: One considers fairness by maximizing the minimum number of well-served users by each RIS without optimizing the phases of the RIS. Similarly, the RISs in this case represent random scatterers.

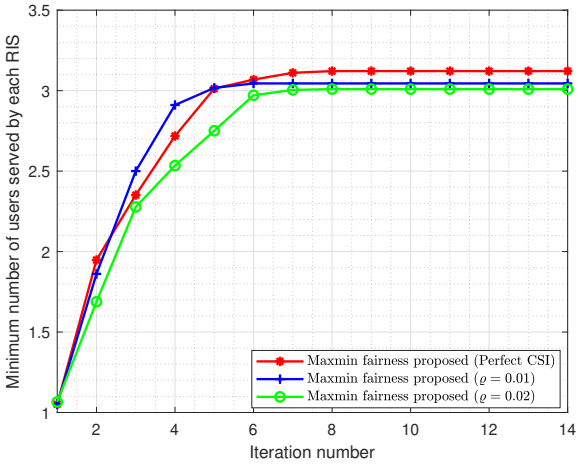

Fig. 3: Minimum number of well-served users by each RIS as a function of the number of iterations.

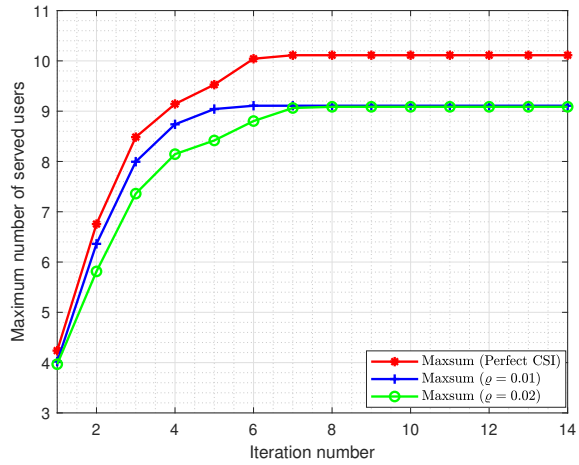

Fig. 4: Maximum number of well-served users as a function of the number of iterations.

Next, we investigate the convergence behavior of the max-min fairness design and the max-sum design. Here, the convergence of the two designs is demonstrated for different channel uncertainty levels set at $\varrho = 0.00, 0.01, \text{and } 0.02$. In this case, $\varrho = 0.00$ represents the case where the CSI is considered to be perfect. We set Γ_k^{th} with values that vary between 3 dB to 10 dB. In this investigation $K = 12$, $M = 9$, $N = 8$, $L = 3$, and $\xi = 3$ dB. Note that we demonstrate the

This article has been accepted for publication in IEEE Transactions on Communications. This is the author's version which has not been fully edited and content may change prior to final publication. Citation information: DOI 10.1109/TCOMM.2025.3525568

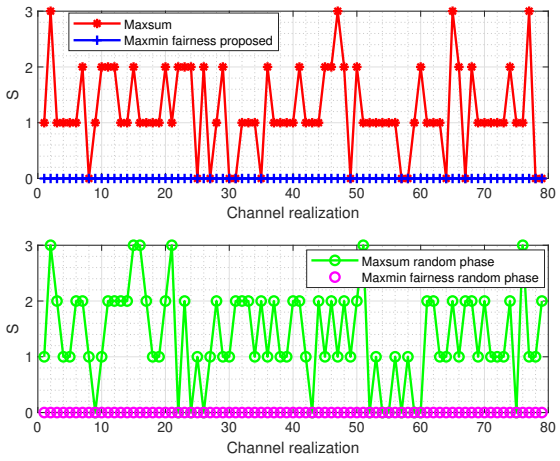

Fig. 5: The difference between the maximum and the minimum number of users well-served per RIS

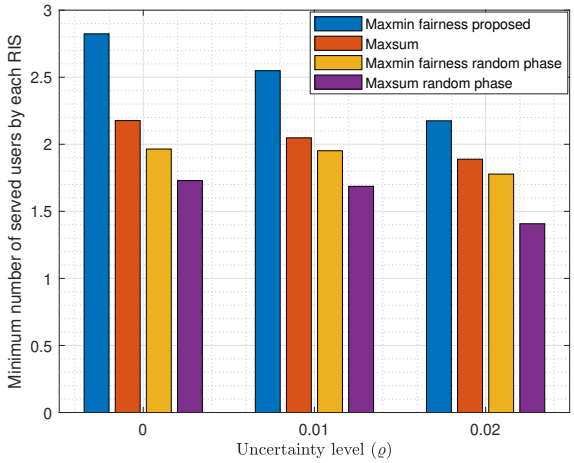

Fig. 6: Average minimum number of well-served users by each RIS as a function of channel error uncertainty level (ϱ)

algorithm convergence within 14 iterations. Firstly, we show the convergence of the proposed design in Fig. 3 where we plot the minimum number of well-served users per each RIS versus the number of iterations. In Fig. 4, we demonstrate the convergence of the max-sum design. Here, we show the maximum number of well-served users as a function of the number of iterations. It is important to note that both schemes converge to a stationary point in about 8 iterations. The cost function for both the max-min fairness (max-min proposed) and the max-sum design increases monotonically until convergence, satisfying the inner approximation properties. Thus, demonstrating that the problems converge to at least a locally optimal solution [74].

In Fig. 5, we show the difference between the maximum and minimum numbers of well-served users per each RIS. Here, the uncertainty level is set at $\varrho = 0.01$, the number of users $K = 12$, the number of RISs $L = 3$, the number of RIS elements is set at $N = 8$ and the number of BS antennas $M = 9$. We set Γ_k^{th} with values that vary between 3 dB to 10 dB. Note that S is the difference between the maximum and the minimum number of well-served users per RIS. The results in Fig. 5 demonstrate that the proposed design provides a more fair and consistent service as compared to the max-sum design. We can see that the difference between the maximum and minimum numbers of well-served users of each RIS is high in some channel realizations for the max-sum scheme. This proves that in some cases very less users are likely to be well-served in certain hotspot areas meaning the users in those locations will be out of coverage. In this case, the proposed design demonstrates its ability to provide fair coverage in different hotspot areas. This is important since customer studies have shown that users value more consistent quality of telecommunication services, rather than burst periods of high and low quality in different hotspot locations [63].

In Fig. 6, we show the minimum number of well-served users by each RIS as a function of channel uncertainty level ϱ. Here $K = 18$, $M = 9$, $N = 8$, $\Gamma_k^{\text{th}} = 6$ dB, $\forall k \in \mathcal{K}$ and the Rician factor is set at 3 dB. Based on the results in Fig. 6, we observe that the max-min fairness proposed design outperforms all the considered benchmark schemes in providing fair coverage. Note that when the CSI is imperfect it becomes highly challenging to serve users with their desired QoS as studied in the previous work [26]. Accordingly, the results in Fig. 6 demonstrate that the design of robust optimization for max-min fairness results in additional flexibility to serve users with their desired QoS under various channel uncertainty levels. In this case, the design ensures that the system is robust to CSI errors. However, note that as the uncertainty level increases, the average minimum number of well-served users generally decreases across all considered schemes. This indicates that higher channel uncertainty negatively impacts the system's ability to provide users with their desired QoS. Additionally, it is worth noting that the schemes with random phases where RISs are deployed as random scatterers result in less performance on average. This demonstrates the importance of RIS phase shift optimization in RIS-assisted networks for improved BF gain.

In Fig. 7, we investigate the impact of varying the number of BS antennas on the minimum number of well-served users of each RIS. Here $K = 18$, M varies between 6 to 12, $\Gamma_k^{\text{th}} = 6$ dB, $\forall k \in \mathcal{K}$ and the Rician factor is set at 3 dB. We set $\varrho = 0.01$. We consider two cases (a) with $N = 8$ and (b) with $N = 16$. In this case, the results demonstrate that increasing the number of antennas increases the number of well-served users by each RIS. Additionally, we note that by increasing the number of RIS elements the average minimum number of well-served users in each hotspot area increases. In this case, we observed that increasing the number of passive RIS elements leads to improved performance gain for a fixed number of active antenna elements at the BS. This is very important since performance gain can be improved in an energy and cost-efficient manner without increasing the number of active elements. In this case, deploying RISs leads to a reduction in energy consumption for powering wireless systems. This is crucial in smart cities as it will help address

This article has been accepted for publication in IEEE Transactions on Communications. This is the author's version which has not been fully edited and content may change prior to final publication. Citation information: DOI 10.1109/TCOMM.2025.3525568

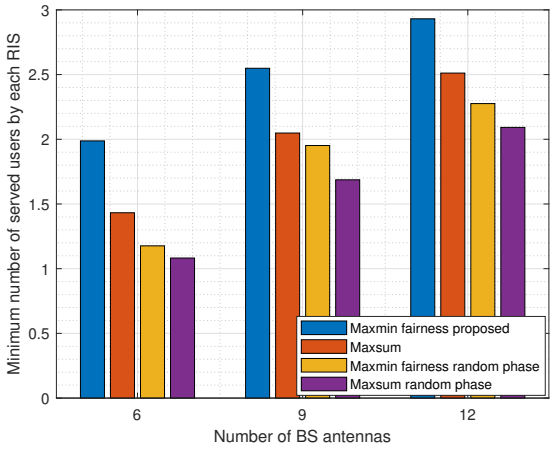

(a) Number of elements per RIS $N = 8$

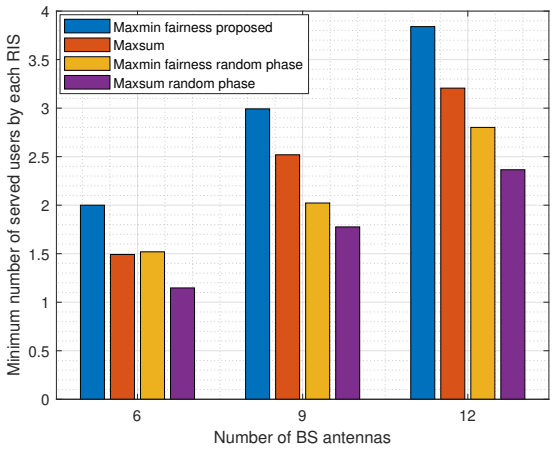

(b) Number of elements per RIS $N = 16$

Fig. 7: Average minimum number of well-served users by each RIS as a function of the number of BS antennas M

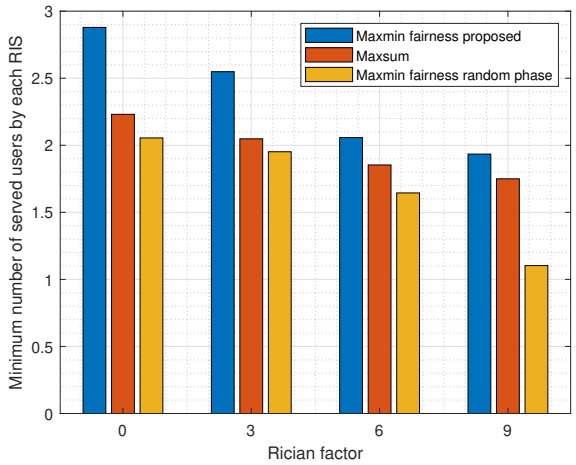

Fig. 8: Average minimum number of well-served users by each RIS as a function of the Rician factor (dB)

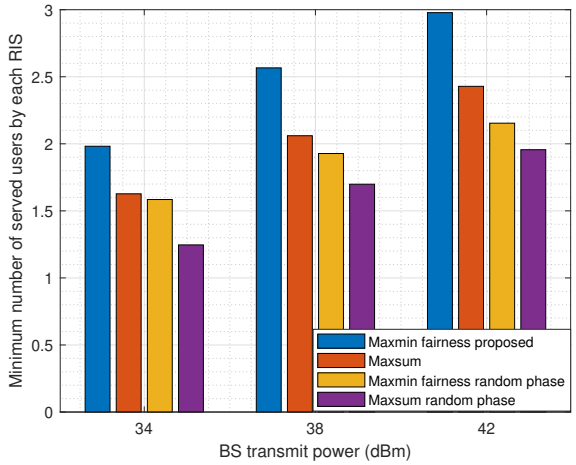

Fig. 9: Average minimum number of well-served users by each RIS as a function of BS transmit power $(P^{\max})$

the ecological concerns raised in various countries regarding the use of fossil fuels [4].

In Fig. 8 we investigate the performance of the considered schemes as a function of the Rician factor. Here $K = 18$, $M = 9$, $N = 8$, $\Gamma_k^{\text{th}} = 6$ dB, $\forall k \in \mathcal{K}$ and we vary the Rician factor between 0 to 9 dB. We set $\varrho = 0.01$. We note that the proposed design results in better performance gain than the max-sum design and the design with random phase. However, the performance gain between the proposed max-min fairness scheme and the max-sum scheme decreases with the increasing Rician factor. This is because in strong LOS propagation, the proposed scheme has fewer combinations than the max-sum scheme, resulting in a more pronounced decrease in the average minimum number of well-served users. Additionally, we note that the minimum number of well-served users per RIS decreases with increasing the Rician factor for all the considered schemes. This is primarily because in strong LOS propagation, the available diversity decreases, making it difficult to generate independent beams with satisfactory signal quality. To further highlight the concept of geographical fairness by comparing the proposed design with the max-sum design using Jain's fairness index. Here, Jain's fairness index can be mathematically modeled as follows as follows: $F_{\text{index}} = \frac{\left(\sum_{\ell=1}^{L} x_\ell\right)^2}{L \cdot \sum_{\ell=1}^{L} x_\ell^2}$, where x_ℓ represents the number of well-served users of each RIS. Note that Jain's fairness index is always equal to 1 for the proposed scheme and around 0.94 for the maxsum scheme with varying the Rician factor. This further demonstrates that the proposed scheme maintains fair access to service to users in different geographical zones.

In Fig. 9 we investigate the performance of the considered scheme as a function of the maximum available power at the BS. Here $K = 18$, $M = 9$, $N = 8$, $\Gamma_k^{\text{th}} = 6$ dB, $\forall k \in \mathcal{K}$ and we vary the BS transmit power between 34 dBm to 42 dBm. The level of channel error uncertainty is set at $\varrho = 0.01$. It is important to note that the proposed design (max-min fairness proposed) provides better performance compared to the relevant benchmark schemes for all the considered power levels. Further, we note that the average minimum number of well-served users by each RIS increases with increasing the

maximum available power at the BS. In this context, increasing the available power at the BS allows the BS to transmit stronger signals thereby providing sufficient resources to meet the minimum QoS requirements for a large number of users. However, we note that with increasing BS transmit power, the performance gap between the max-min fairness proposed scheme and the max-sum scheme in terms of the average minimum number of well-served users per RIS increases. In this case, increasing the available transmit power at the BS does not necessarily improve geographical fairness. Instead, the results demonstrate that with increased power levels, the BS tends to favor or allocate more power to users closer to the RIS with favorable conditions thereby resulting in less performance of the max-sum design in certain locations. Thus, the max-sum design becomes more unfair to users in certain hotspot areas.

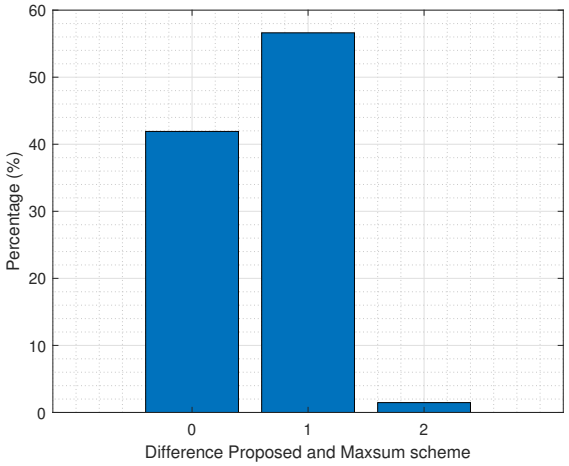

Fig. 10: Difference in the minimum number of well-served users in proximity to each RIS between the proposed scheme and the max-sum scheme as a percentage of channel realizations

In Fig. 10, we present the difference in the minimum number of well-served users in proximity to each RIS between the proposed and the max-sum schemes as a percentage over a number of channel realizations. Here, the results show a load imbalance in some channel realizations between the two schemes. Specifically, the max-sum scheme is unfair 58% of the realizations with around 2% worst-case scenario where there is a difference of 2 users between the two schemes. In this work, we consider 9 BS antennas and 3 RISs. Accordingly, the worst-case scenario highlights that at most 1 user is likely to be served in one of the hotspot areas with the max-sum scheme, thus, an increased chance that the hotspot will be left out of coverage. Note that this performance is likely to vary depending on the scenario and the system setup.

Overall, it is apparent that the robust max-min fairness resource allocation design results in more geographically fair coverage or service to users in different hotspot areas despite the availability of unfair geographical locations. The gain of the proposed design varies based on the considered scenario and several system parameters including the number of antennas, the number of RIS elements, the level of channel error uncertainty, the total available power at the BS, and the Rician factor.

VI. Conclusions

This work solved the robust fairness problem to ensure geographical fairness in multi-RIS-assisted networks. Specifically, we formulate an optimization problem to maximize the minimum expected number of well-served users in proximity to each RIS while considering the total available transmit power at the BS and the worst-case QoS constraints. The resulting problem is a MINLP which is highly challenging to solve efficiently. Thus, a practical AO algorithm was proposed to handle the robust max-min fairness resource allocation design. To address the semi-infinite channel uncertainty constraints within the bounded CSI error model framework, we resorted to the S-procedure (S-Lemma) and general sign-definiteness. Simulation results demonstrated that the proposed design outperforms all the considered benchmark schemes in providing fair coverage for different system settings. Notably, the proposed design results in a more fair and consistent service in all hotspot areas supported by distributed RISs compared to the max-sum scheme and the scheme with random phases. Specifically, maximizing the sum of well-served users of all RIS in a multi-RIS-assisted network results in inconsistent service in some geographical locations. Accordingly, this study demonstrated the importance of ensuring geographical fairness through the robust max-min fairness design compared to the robust max-sum design which focuses on maximizing the sum of well-served users without considering consistent and reliable service availability in different geographical locations. Additionally, results demonstrate the flexibility provided by the robust optimization design in serving users with their desired QoS in different hotspot areas under various channel uncertainty levels.

Due to the complexity of the proposed design, future work will resort to deep learning techniques for channel estimation and solving the highly challenging optimization problem, especially in dynamic environments.

Appendix

For a complex scalar variable y and variable t, the first-order Taylor approximation is given as follows $\frac{|y|^2}{t} \geq \frac{2\Re\{y^{*,(\iota)}y\}}{t^{(\iota)}} - \frac{y^{*,(\iota)}y^{(\iota)}}{(t^{(\iota)})^2}t^{(\iota)}$. For the Base-Station Precoding Design subproblem, by substituting y, $y^{(\iota)}$, t and $t^{(\iota)}$ with $|(\mathbf{h}_k^H + \sum_{\ell\in\mathcal{L}}\psi_{k,\ell}\boldsymbol{\phi}_\ell^H\mathbf{H}_{\ell,k})\mathbf{w}_k|^2$, $|(\mathbf{h}_k^H + \sum_{\ell\in\mathcal{L}}\psi_{k,\ell}\boldsymbol{\phi}_\ell^H\mathbf{H}_{\ell,k})\mathbf{w}_k^{(\iota)}|^2$, η_k and $\eta_k^{(\iota)}$, respectively, we obtain

$$
\begin{aligned}
&\frac{|(\mathbf{h}_k^H + \sum_{\ell\in\mathcal{L}}\psi_{k,\ell}\boldsymbol{\phi}_\ell^H\mathbf{H}_{\ell,k})\mathbf{w}_k|^2}{\eta_k} \\
&\geq 2\,\mathrm{Re}\left\{\left(\mathbf{h}_k^{\mathrm{H}} + \sum_{\ell\in\mathcal{L}}\psi_{\ell,k}\boldsymbol{\phi}_\ell^{\mathrm{H}}\left(\hat{\mathbf{H}}_{\ell,k} + \boldsymbol{\Psi}_{\ell,k}\right)\right)\mathbf{w}_k^{(\iota)}\mathbf{w}_k^{\mathrm{H}}\right. \\
&\left.\left(\mathbf{h}_k + \sum_{\ell\in\mathcal{L}}\psi_{\ell,k}\left(\hat{\mathbf{H}}_{\ell,k} + \boldsymbol{\Psi}_{\ell,k}\right)\boldsymbol{\phi}_\ell\right)\right\}(\eta_k^{(\iota)})^{-1} \\
&- \left(\mathbf{h}_k^{\mathrm{H}} + \sum_{\ell\in\mathcal{L}}\psi_{\ell,k}\boldsymbol{\phi}_\ell^{\mathrm{H}}\left(\hat{\mathbf{H}}_{\ell,k} + \boldsymbol{\Psi}_{\ell,k}\right)\right)\mathbf{w}_k^{(\iota)}\mathbf{w}_k^{(\iota),\mathrm{H}}
\end{aligned}
$$

$$\left(\mathbf{h}_k + \sum_{\ell\in\mathcal{L}} \psi_{\ell,k}\left(\hat{\mathbf{H}}_{\ell,k} + \mathbf{\Psi}_{\ell,k}\right)\boldsymbol{\phi}_\ell\right)\eta_k(\eta_k^{(\iota)})^{-2}. \tag{43}$$

For the Passive RIS-BF Design subproblem, by substituting y, $y^{(\iota)}$, t and $t^{(\iota)}$ with $|(\mathbf{h}_k^H + \sum_{\ell\in\mathcal{L}} \psi_{k,\ell}\boldsymbol{\phi}_\ell^H\mathbf{H}_{\ell,k})\mathbf{w}_k|^2$, $|(\mathbf{h}_k^H + \sum_{\ell\in\mathcal{L}} \psi_{k,\ell}\boldsymbol{\phi}_\ell^{(\iota),H}\mathbf{H}_{\ell,k})\mathbf{w}_k|^2$, η_k and $\eta_k^{(\iota)}$, respectively, we obtain

$$\begin{aligned}
&\frac{|(\mathbf{h}_k^H + \sum_{\ell\in\mathcal{L}} \psi_{k,\ell}\boldsymbol{\phi}_\ell^H\mathbf{H}_{\ell,k})\mathbf{w}_k|^2}{\eta_k} \\
&\geq 2\,\mathrm{Re}\Bigg\{\left(\mathbf{h}_k^{\mathrm{H}} + \sum_{\ell\in\mathcal{L}} \psi_{\ell,k}\boldsymbol{\phi}_\ell^{(\iota),\mathrm{H}}\left(\hat{\mathbf{H}}_{\ell,k} + \mathbf{\Psi}_{\ell,k}\right)^H\right) \\
&\mathbf{w}_k\mathbf{w}_k^{\mathrm{H}}\left(\mathbf{h}_k + \sum_{\ell\in\mathcal{L}} \psi_{\ell,k}\left(\hat{\mathbf{H}}_{\ell,k} + \mathbf{\Psi}_{\ell,k}\right)^H\boldsymbol{\phi}_\ell\right)\Bigg\}(\eta_k^{(\iota)})^{-1} \\
&- \left(\mathbf{h}_k^{\mathrm{H}} + \sum_{\ell\in\mathcal{L}} \psi_{\ell,k}\boldsymbol{\phi}_\ell^{(\iota),\mathrm{H}}\left(\hat{\mathbf{H}}_{\ell,k} + \mathbf{\Psi}_{\ell,k}\right)\right)\mathbf{w}_k\mathbf{w}_k^{\mathrm{H}} \\
&\left(\mathbf{h}_k + \sum_{\ell\in\mathcal{L}} \psi_{\ell,k}\left(\hat{\mathbf{H}}_{\ell,k} + \mathbf{\Psi}_{\ell,k}\right)^H\boldsymbol{\phi}_\ell^{(\iota)}\right)\eta_k(\eta_k^{(\iota)})^{-2}.
\end{aligned} \tag{44}$$

Note that $\mathbf{H}_{\ell,k} = \hat{\mathbf{H}}_{\ell,k} + \mathbf{\Psi}_{\ell,k}$. Accordingly, using mathematical transformations i.e $\mathrm{Tr}\left(\mathbf{A}^{\mathrm{H}}\mathbf{B}\right) = \mathrm{vec}^{\mathrm{T}}(\mathbf{A})\,\mathrm{vec}(\mathbf{B})$ and $\mathrm{Tr}(\mathbf{ABCD}) = \left(\mathrm{vec}^{\mathrm{T}}(\mathbf{D})\right)^{\mathrm{T}} \otimes \left(\mathbf{C}^{\mathrm{T}} \otimes \mathbf{A}\right)\mathrm{vec}(\mathbf{B})$ [76], the expression on the right-hand side of (43) and (44) for the precoding design and the RIS phase shift design can be expanded to obtain the linear approximation function for the precoding and RIS phase shift worst-case useful signal power, respectively. Hence, end of proof.

REFERENCES

[1] P. Zivuku, S. Kisseleff, K. Ntontin, A. K. Papazafeiropoulos, A. B. Mohammad Adam, S. Chatzinotas, and B. Ottersten, "Resource allocation for geographical fairness in multi-RIS-aided outdoor-to-indoor communications," in *ICC 2024 - IEEE Int. Conf. Commun.*, 2024, pp. 3420–3426.

[2] M. Agiwal, A. Roy, and N. Saxena, "Next generation 5G wireless networks: A comprehensive survey," *IEEE Commun. Surv. Tutorials*, vol. 18, no. 3, pp. 1617–1655, 2016.

[3] L. U. Khan, I. Yaqoob, M. Imran, Z. Han, and C. S. Hong, "6G wireless systems: A vision, architectural elements, and future directions," *IEEE access*, vol. 8, pp. 147 029–147 044, 2020.

[4] S. Kisseleff, W. A. Martins, H. Al-Hraishawi, S. Chatzinotas, and B. Ottersten, "Reconfigurable intelligent surfaces for smart cities: Research challenges and opportunities," *EEE Open J. Commun. Soc.*, vol. 1, pp. 1781–1797, 2020.

[5] B. N. Silva, M. Khan, and K. Han, "Towards sustainable smart cities: A review of trends, architectures, components, and open challenges in smart cities," *Sustainable Cities Soc.*, vol. 38, pp. 697–713, 2018.

[6] E. Basar, M. Di Renzo, J. De Rosny, M. Debbah, M.-S. Alouini, and R. Zhang, "Wireless communications through reconfigurable intelligent surfaces," *IEEE Access*, vol. 7, pp. 116 753–116 773, 2019.

[7] Y. Liu, X. Liu, X. Mu, T. Hou, J. Xu, M. Di Renzo, and N. Al-Dhahir, "Reconfigurable intelligent surfaces: Principles and opportunities," *IEEE Commun. Surv. Tutorials*, vol. 23, no. 3, pp. 1546–1577, 2021.

[8] R. Liu, Q. Wu, M. Di Renzo, and Y. Yuan, "A path to smart radio environments: An industrial viewpoint on reconfigurable intelligent surfaces," *IEEE Wireless Commun.*, vol. 29, no. 1, pp. 202–208, 2022.

[9] A. Adam, M. A. Ouamri, M. S. A. Muthanna, X. Li, M. A. Elhassan, and A. Muthanna, "Real-time and security-aware precoding in RIS-empowered multi-user wireless networks," *arXiv preprint arXiv:2401.00192*, 2023.

[10] M. Di Renzo, K. Ntontin, J. Song, F. H. Danufane, X. Qian, F. Lazarakis, J. De Rosny, D.-T. Phan-Huy, O. Simeone, R. Zhang *et al.*, "Reconfigurable intelligent surfaces vs. relaying: Differences, similarities, and performance comparison," *IEEE Open J. Commun. Soc.*, vol. 1, pp. 798–807, 2020.

[11] Q. Wu, S. Zhang, B. Zheng, C. You, and R. Zhang, "Intelligent reflecting surface-aided wireless communications: A tutorial," *IEEE Trans. Commun.*, vol. 69, no. 5, pp. 3313–3351, 2021.

[12] T. Ji, M. Hua, C. Li, Y. Huang, and L. Yang, "Robust max-min fairness transmission design for IRS-aided wireless network considering user location uncertainty," *IEEE Trans. Commun.*, 2023.

[13] P. Wang, J. Fang, X. Yuan, Z. Chen, and H. Li, "Intelligent reflecting surface-assisted millimeter wave communications: Joint active and passive precoding design," *IEEE Trans. Veh. Technol.*, vol. 69, no. 12, pp. 14 960–14 973, 2020.

[14] M. D. Renzo, M. Debbah, D.-T. Phan-Huy, A. Zappone, M.-S. Alouini, C. Yuen, V. Sciancalepore, G. C. Alexandropoulos, J. Hoydis, H. Gacanin *et al.*, "Smart radio environments empowered by reconfigurable AI meta-surfaces: An idea whose time has come," *EURASIP J. Wireless Commun. Networking*, vol. 2019, no. 1, pp. 1–20, 2019.

[15] M. Di Renzo, A. Zappone, M. Debbah, M.-S. Alouini, C. Yuen, J. de Rosny, and S. Tretyakov, "Smart radio environments empowered by reconfigurable intelligent surfaces: How it works, state of research, and the road ahead," *IEEE J. Sel. Areas Commun.*, vol. 38, no. 11, pp. 2450–2525, 2020.

[16] C. Pan, G. Zhou, K. Zhi, S. Hong, T. Wu, Y. Pan, H. Ren, M. D. Renzo, A. Lee Swindlehurst, R. Zhang, and A. Y. Zhang, "An overview of signal processing techniques for RIS/IRS-aided wireless systems," *IEEE J. Sel. Top. Signal Process.*, vol. 16, no. 5, pp. 883–917, 2022.

[17] D. Xu, X. Yu, Y. Sun, D. W. K. Ng, and R. Schober, "Resource allocation for secure IRS-assisted multiuser MISO systems," in *2019 IEEE Globecom Workshops (GC Wkshps)*. IEEE, 2019, pp. 1–6.

[18] A. Almohamad, A. M. Tahir, A. Al-Kababji, H. M. Furqan, T. Khattab, M. O. Hasna, and H. Arslan, "Smart and secure wireless communications via reflecting intelligent surfaces: A short survey," *IEEE Open J. Commun. Soc.*, vol. 1, pp. 1442–1456, 2020.

[19] B. Feng, J. Gao, Y. Wu, W. Zhang, X.-G. Xia, and C. Xiao, "Optimization techniques in reconfigurable intelligent surface aided networks," *IEEE Wireless Commun.*, vol. 28, no. 6, pp. 87–93, 2021.

[20] P. Zivuku, S. Kisseleff, W. A. Martins, H. Al-Hraishawi, S. Chatzinotas, and B. Ottersten, "Performance of joint symbol level precoding and RIS phase shift design in the finite block length regime with constellation rotation," in *2023 IEEE 34th Annual Int. Symp. Pers. Indoor Mob. Radio Commun. (PIMRC)*, 2023, pp. 1–6.

[21] C. Huang, A. Zappone, G. C. Alexandropoulos, M. Debbah, and C. Yuen, "Reconfigurable intelligent surfaces for energy efficiency in wireless communication," *IEEE Trans. Wireless Commun.*, vol. 18, no. 8, pp. 4157–4170, 2019.

[22] Y. Gao, C. Yong, Z. Xiong, D. Niyato, Y. Xiao, and J. Zhao, "Reconfigurable intelligent surface for MISO systems with proportional rate constraints," in *ICC 2020 - 2020 IEEE Int. Conf. Commun. (ICC)*, 2020, pp. 1–7.

[23] H. Guo, Y.-C. Liang, J. Chen, and E. G. Larsson, "Weighted sum-rate maximization for reconfigurable intelligent surface aided wireless networks," *IEEE Trans. Wireless Commun.*, vol. 19, no. 5, pp. 3064–3076, 2020.

[24] H. Zhang, S. Ma, Z. Shi, X. Zhao, and G. Yang, "Sum-rate maximization of RIS-aided multi-user MIMO systems with statistical CSI," *IEEE Trans. Wireless Commun.*, 2022.

[25] X. Li, Z. Xie, G. Huang, J. Zhang, M. Zeng, and Z. Chu, "Sum rate maximization for RIS-aided NOMA with direct links," *IEEE Networking Lett.*, vol. 4, no. 2, pp. 55–58, 2022.

[26] P. Zivuku, S. Kisseleff, V.-D. Nguyen, W. A. Martins, K. Ntontin, S. Chatzinotas, and B. Ottersten, "Joint RIS-aided precoding and multislot scheduling for maximum user admission in smart cities," *IEEE Trans. Commun.*, vol. 72, no. 1, pp. 418–433, 2024.

[27] P. Zivuku, S. Kisseleff, V.-D. Nguyen, K. Ntontin, W. A. Martins, S. Chatzinotas, and B. Ottersten, "Maximizing the number of served users in a smart city using reconfigurable intelligent surfaces," in *2022 IEEE Wireless Commun. Net. Conf. (WCNC)*, 2022, pp. 494–499.

[28] H. Gao, K. Cui, C. Huang, and C. Yuen, "Robust beamforming for RIS-assisted wireless communications with discrete phase shifts," *IEEE Wireless Commun. Lett.*, vol. 10, no. 12, pp. 2619–2623, 2021.

[29] M. Gao, J. Yang, H. Li, and Y. Wang, "Robust beamforming optimization design for RIS-aided MIMO systems with practical phase shift model and imperfect CSI," *IEEE Internet Things J.*, 2023.

[30] Z. Peng, Z. Chen, C. Pan, G. Zhou, and H. Ren, "Robust transmission design for RIS-aided communications with both transceiver hardware impairments and imperfect CSI," *IEEE Wireless Commun. Lett.*, vol. 11, no. 3, pp. 528–532, 2021.

[31] J. Wang, S. Gong, Q. Wu, and S. Ma, "RIS-aided MIMO systems with hardware impairments: Robust beamforming design and analysis," *IEEE Trans. Wireless Commun.*, 2023.

[32] G. Zhou, C. Pan, H. Ren, K. Wang, M. D. Renzo, and A. Nallanathan, "Robust beamforming design for intelligent reflecting surface aided MISO communication systems," *IEEE Wireless Commun. Lett.*, vol. 9, no. 10, pp. 1658–1662, 2020.

[33] K. Xu, S. Gong, M. Cui, G. Zhang, and S. Ma, "Statistically robust transceiver design for multi-RIS assisted multi-user mimo systems," *IEEE Commun. Lett.*, vol. 26, no. 6, pp. 1428–1432, 2022.

[34] A. Taha, M. Alrabeiah, and A. Alkhateeb, "Enabling large intelligent surfaces with compressive sensing and deep learning," *IEEE access*, vol. 9, pp. 44 304–44 321, 2021.

[35] G. Zhou, C. Pan, H. Ren, K. Wang, and A. Nallanathan, "A framework of robust transmission design for IRS-aided MISO communications with imperfect cascaded channels," *IEEE Trans. Signal Process.*, vol. 68, pp. 5092–5106, 2020.

[36] P. Wang, J. Fang, H. Duan, and H. Li, "Compressed channel estimation for intelligent reflecting surface-assisted millimeter wave systems," *IEEE Signal Process Lett.*, vol. 27, pp. 905–909, 2020.

[37] Z. Yang, M. Chen, W. Saad, W. Xu, M. Shikh-Bahaei, H. V. Poor, and S. Cui, "Energy-efficient wireless communications with distributed reconfigurable intelligent surfaces," *IEEE Trans. Wireless Commun.*, vol. 21, no. 1, pp. 665–679, 2022.

[38] Q. Sun, Y. Wu, X. Chen, and J. Zhang, "SLNR-based joint RIS-UE association and beamforming design for multi-RIS aided wireless communications," *IEEE Trans. Veh. Technol.*, pp. 1–11, 2024.

[39] T. V. Nguyen, D. N. Nguyen, M. D. Renzo, and R. Zhang, "Leveraging secondary reflections and mitigating interference in multi-IRS/RIS aided wireless networks," *IEEE Trans. Wireless Commun.*, vol. 22, no. 1, pp. 502–517, 2023.

[40] M. W. Shabir, T. N. Nguyen, J. Mirza, B. Ali, and M. A. Javed, "Transmit and reflect beamforming for max-min SINR in IRS-aided MIMO vehicular networks," *IEEE Trans. Intell. Transp. Syst.*, vol. 24, no. 1, pp. 1099–1105, 2022.

[41] Z. Zhao, Z. Yang, C. Huang, L. Wei, Q. Yang, C. Zhong, W. Xu, and Z. Zhang, "A joint communication and computation design for distributed RIS-assisted probabilistic semantic communication in IIoT," *IEEE Internet Things J.*, vol. 11, no. 16, pp. 26 568–26 579, 2024.

[42] Z. Li, M. Hua, Q. Wang, and Q. Song, "Weighted sum-rate maximization for multi-IRS aided cooperative transmission," *IEEE Wire. Commun. Lett.*, vol. 9, no. 10, pp. 1620–1624, 2020.

[43] M. A. Saeidi, M. J. Emadi, H. Masoumi, M. R. Mili, D. W. K. Ng, and I. Krikidis, "Weighted sum-rate maximization for multi-IRS-assisted full-duplex systems with hardware impairments," *IEEE Trans. Cognit. Commun. Networking*, vol. 7, no. 2, pp. 466–481, 2021.

[44] Y. Gao, J. Xu, W. Xu, D. W. K. Ng, and M.-S. Alouini, "Distributed IRS with statistical passive beamforming for MISO communications," *IEEE Wire. Commun. Lett.*, vol. 10, no. 2, pp. 221–225, 2021.

[45] T. N. Do, G. Kaddoum, T. L. Nguyen, D. B. Da Costa, and Z. J. Haas, "Multi-RIS-aided wireless systems: Statistical characterization and performance analysis," *IEEE Trans. Commun.*, vol. 69, no. 12, pp. 8641–8658, 2021.

[46] Z. Zhang and Z. Zhao, "Weighted sum-rate maximization for multi-hop RIS-aided multi-user communications: A minorization-maximization approach," in *2021 IEEE 22nd IEEE Workshop Signal Process. Adv. Wirel. Commun. SPAWC*, 2021, pp. 106–110.

[47] Z. Yang, M. Chen, W. Saad, W. Xu, M. Shikh-Bahaei, H. V. Poor, and S. Cui, "Energy-efficient wireless communications with distributed reconfigurable intelligent surfaces," *IEEE Trans. Wire. Commun.*, vol. 21, no. 1, pp. 665–679, 2021.

[48] E. Matskani, N. D. Sidiropoulos, Z.-q. Luo, and L. Tassiulas, "Convex approximation techniques for joint multiuser downlink beamforming and admission control," *IEEE Trans. Wireless Commun.*, vol. 7, no. 7, pp. 2682–2693, 2008.

[49] E. M. Mohamed, S. Hashima, K. Hatano, E. Takimoto, and M. Abdel-Nasser, "Load balancing multi-player MAB approaches for RIS-aided mmwave user association," *IEEE Access*, vol. 11, pp. 15 816–15 830, 2023.

[50] S. He, J. Yuan, Z. An, Y. Yi, and Y. Huang, "Maximizing the set cardinality of users scheduled for ultra-dense uRLLC networks," *IEEE Commun. Lett.*, vol. 25, no. 12, pp. 3952–3955, 2021.

[51] R. Kaliski and Y.-H. Han, "Socially Aware V2X Localized QoS," *EEE Internet Things J.*, vol. 11, no. 15, pp. 25 925–25 938, 2024.

[52] Q. Wu and R. Zhang, "Beamforming optimization for wireless network aided by intelligent reflecting surface with discrete phase shifts," *IEEE Trans. Commun.*, vol. 68, no. 3, pp. 1838–1851, 2020.

[53] L. Zheng, Y.-W. P. Hong, C. W. Tan, C.-L. Hsieh, and C.-H. Lee, "Wireless Max–Min Utility Fairness With General Monotonic Constraints by Perron–Frobenius Theory," *IEEE Trans. Inf. Theory*, vol. 62, no. 12, pp. 7283–7298, 2016.

[54] C. E. Kontokosta and B. Hong, "Bias in smart city governance: How socio-spatial disparities in 311 complaint behavior impact the fairness of data-driven decisions," *Sustainable Cities Soc.*, vol. 64, p. 102503, 2021.

[55] Y. Zhang, T. Zhao, and S. Elmalaki, "Towards Fairness-aware Crowd Management System and Surge Prevention in Smart Cities," in *2024 IEEE Workshop on Design Automation for CPS and IoT (DESTION)*, 2024, pp. 46–54.

[56] S. Musa, "Smart Cities-A Road Map for Development," *IEEE Potentials*, vol. 37, no. 2, pp. 19–23, 2018.

[57] Y. Liu, X. Liu, X. Mu, T. Hou, J. Xu, M. Di Renzo, and N. Al-Dhahir, "Reconfigurable Intelligent Surfaces: Principles and Opportunities," *IEEE Commun. Surv. Tutorials*, vol. 23, no. 3, pp. 1546–1577, 2021.

[58] N. Alliance, "6G drivers and vision," *version*, vol. 1, p. 19, 2021.

[59] Q. Wu, B. Zheng, C. You, L. Zhu, K. Shen, X. Shao, W. Mei, B. Di, H. Zhang, E. Basar *et al.*, "Intelligent surfaces empowered wireless network: Recent advances and the road to 6G," *Proc. IEEE*, 2024.

[60] Huawei, "Ubiquitous connectivity forges an intelligent future," Huawei Technologies Co., Ltd., Tech. Rep., 2021. [Online]. Available: https://www-file.huawei.com/-/media/corporate/pdf/public-policy/ubiquitous_connectivity_forges_an_intelligent_future_en.pdf

[61] D. E. Okonta and V. Vukovic, "Smart cities software applications for sustainability and resilience," *Heliyon*, vol. 10, no. 12, 2024.

[62] E. Björnson, J. Hoydis, L. Sanguinetti *et al.*, "Massive MIMO networks: Spectral, energy, and hardware efficiency," *Foundations and Trends® in Signal Processing*, vol. 11, no. 3-4, pp. 154–655, 2017.

[63] Ericsson, "Ericsson mobility report 2024," Ericsson, Tech. Rep., 2024. [Online]. Available: http://www.ericsson.com/mobility-report

[64] B. Yang, X. Cao, C. Huang, C. Yuen, M. Di Renzo, Y. L. Guan, D. Niyato, L. Qian, and M. Debbah, "Federated spectrum learning for reconfigurable intelligent surfaces-aided wireless edge networks," *IEEE Trans. Wireless Commun.*, vol. 21, no. 11, pp. 9610–9626, 2022.

[65] X. Mu, Y. Liu, L. Guo, J. Lin, and R. Schober, "Simultaneously transmitting and reflecting (STAR) RIS aided wireless communications," *IEEE Trans. Wireless Commun.*, vol. 21, no. 5, pp. 3083–3098, 2021.

[66] G. Zhou, C. Pan, H. Ren, K. Wang, and M. D. Renzo, "Fairness-oriented multiple RIS-aided mmwave transmission: Stochastic optimization methods," *IEEE Trans. Signal Process*, vol. 70, pp. 1402–1417, 2022.

[67] E. A. Gharavol and E. G. Larsson, "The sign-definiteness lemma and its applications to robust transceiver optimization for multiuser MIMO systems," *IEEE Trans. on Signal Processing*, vol. 61, no. 2, pp. 238–252, 2013.

[68] S. Boyd, L. El Ghaoui, E. Feron, and V. Balakrishnan, *Linear matrix inequalities in system and control theory*. SIAM, 1994.

[69] A. B. M. Adam, X. Wan, M. A. M. Elhassan, M. S. A. Muthanna, A. Muthanna, N. Kumar, and M. Guizani, "Intelligent and robust UAV-aided multiuser RIS communication technique with jittering UAV and imperfect hardware constraints," *IEEE Trans. Veh. Technol.*, vol. 72, no. 8, pp. 10 737–10 753, 2023.

[70] I. R. Petersen, "A stabilization algorithm for a class of uncertain linear systems," *Syst. Control Lett.*, vol. 8, no. 4, pp. 351–357, 1987.

[71] E. Che, H. D. Tuan, and H. H. Nguyen, "Joint optimization of cooperative beamforming and relay assignment in multi-user wireless relay networks," *IEEE Trans. Wireless Commun.*, vol. 13, no. 10, pp. 5481–5495, 2014.

[72] S. P. Boyd and L. Vandenberghe, *Convex optimization*. Cambridge UP, 2004.

[73] M. Grant and S. Boyd, "CVX: Matlab software for disciplined convex programming, version 2.1," 2014.

[74] B. R. Marks and G. P. Wright, "A general inner approximation algorithm for nonconvex mathematical programs," *Operations research*, vol. 26, no. 4, pp. 681–683, 1978.

[75] A. Ben-Tal and A. Nemirovski, *Lectures on modern convex optimization: analysis, algorithms, and engineering applications*. SIAM, 2001.

[76] X.-D. Zhang, *Matrix analysis and applications*. Cambridge UP, 2017.

This article has been accepted for publication in IEEE Transactions on Communications. This is the author's version which has not been fully edited and content may change prior to final publication. Citation information: DOI 10.1109/TCOMM.2025.3525568

Progress Zivuku (Graduate Student Member, IEEE) received her B.Sc. degree in Telecommunications engineering at the University of Tlemcen, Algeria, in 2018 and her M.Sc. degree in information and communication engineering at the University of Trento, Italy, in 2020. She is currently working towards a Ph.D. degree with the SIGCOM Group in the Interdisciplinary Centre for Security, Reliability and Trust (SnT), University of Luxembourg. Her research interests include but are not limited to reconfigurable intelligent surfaces (RIS), joint communication and sensing, resource allocation, signal processing, optimization algorithms for future wireless networks, and cooperative communications.

Abuzar B. M. Adam (Member, IEEE) received the M.Eng. degree in computer science and technology from Xiamen University, Xiamen, China, in 2017, and the Ph.D. degree from Chongqing University of Posts and Telecommunications, Chongqing, China, in 2021. He was a Postdoctoral Fellow and a Lecturer with the School of Communications and Information Engineering. He was a Research Assistant Professor with the Institute of Next-Generation Networks, Chongqing University of Posts and Telecommunications. He is currently a Research Associate with the Interdisciplinary Centre for Security, Reliability and Trust (SnT), University of Luxembourg, Luxembourg. His research interests include AI-enabled wireless networks, RIS-assisted wireless networks, integrated terrestrial/non-terrestrial networks, convex optimization, and machine learning and applications. He was a recipient of the 2021 Outstanding Doctoral Student Award

Konstantinos Ntontin (Member, IEEE) received the Diploma degree in electrical and computer engineering from the University of Patras, Greece, in 2006, the M.Sc. degree in wireless systems from the Royal Institute of Technology (KTH), Sweden, in 2009, and the Ph.D. degree from the Technical University of Catalonia, Spain, in 2015. He is currently a Research Scientist with the SIGCOM Research Group at SnT, University of Luxembourg. In the past, he held research associate positions with the Electronic Engineering and Telecommunications Department, University of Barcelona, the Informatics and Telecommunications Department, University of Athens, and the National Centre of Scientific Research-"Demokritos." In addition, he held an internship position with Ericsson Eurolab Gmbh, Germany. His research interests are related to the physical layer of wireless telecommunications with focus on performance analysis in fading channels, MIMO systems, array beamforming, transceiver design, and stochastic modeling of wireless channels.

Steven Kisseleff (S'12, M'17, SM'22) received his M.Sc. degree in Information Technology from the Technical University of Kaiserslautern, Germany, and Ph.D. in Electrical Engineering from the Friedrich-Alexander University of Erlangen-Nurnberg (FAU), Germany in 2011 and 2017, respectively. From 2018 to 2023, he was with the SIGCOM Research Group at SnT, University of Luxembourg, at first as Research Associate and then as Research Scientist. In 2023, Dr. Kisseleff joined the Fraunhofer Institute for Integrated Circuits (IIS), Germany, where he currently holds a Senior Scientist position. His research interests include design and optimization of satellite networks, multi-antenna systems and internet of things.

Vu Nguyen Ha (Senior Member, IEEE) received the B.Eng. degree (Hons.) from the French Training Program for Excellent Engineers in Vietnam, Ho Chi Minh City University of Technology, Vietnam, the Addendum degree from the École Nationale Supérieure des Télécommunications de BretagneGroupe des École des Télécommunications, Bretagne, France, in 2007, and the Ph.D. degree (Hons.) from the Institut National de la Recherche Scientifique-Énergie, Matériaux et Télécommunications, Université du Québec, Montreal, QC, Canada, in 2017. From 2016 to 2021, he worked as a Postdoctoral Fellow with the Ecole Polytechnique de Montreal, and then the Resilient Machine Learning Institute, École de Technologie Supérieure, University of Québec. He is currently a Research Scientist with the Interdisciplinary Centre for Security, Reliability, and Trust, University of Luxembourg. His research interests include applying/developing optimization and machine-learning-based solution for RRM problems in MAC/PHY layers of several wireless communication systems, including SATCOM, 5G/beyond-5G, HetNets, Cloud RAN, massive MIMO, mobileedge computing, and 802.11ax WiFi. He received the Innovation Award for his Ph.D. degree. He was a recipient of the FRQNT Postdoctoral Fellowship for International Researcher (PBEEE) awarded by the Québec Ministry of Education, Canada, in 2018 and 2019. In 2021 and 2022, he was also awarded the Certificate for Exemplary Reviews by the IEEE WIRELESS COMMUNICATIONS LETTERS.

Symeon Chatzinotas (MEng, MSc, PhD, FIEEE) is currently Full Professor / Chief Scientist I and Head of the research group SIGCOM in the Interdisciplinary Centre for Security, Reliability and Trust, University of Luxembourg. In parallel, he is an Adjunct Professor in the Department of Electronic Systems, Norwegian University of Science and Technology and a Collaborating Scholar of the Institute of Informatics & Telecommunications, National Center for Scientific Research "Demokritos".

In the past, he has lectured as a Visiting Professor at the University of Parma, Italy and contributed in numerous R&D projects for the Institute of Telematics and Informatics, Center of Research and Technology Hellas and Mobile Communications Research Group, Center of Communication Systems Research, University of Surrey.

He has received the M.Eng. in Telecommunications from Aristotle University of Thessaloniki, Greece and the M.Sc. and Ph.D. in Electronic Engineering from University of Surrey, UK in 2003, 2006 and 2009 respectively.

He has authored more than 800 technical papers in refereed international journals, conferences and scientific books and has received numerous awards and recognitions, including the IEEE Fellowship and an IEEE Distinguished Contributions Award. He is currently in the editorial board of the IEEE Transactions on Communications, IEEE Open Journal of Vehicular Technology and the International Journal of Satellite Communications and Networking.

Björn Ottersten (S'87–M'89–SM'99–F'04) received the M.S. degree in electrical engineering and applied physics from Linköping University, Linköping, Sweden, in 1986, and the Ph.D. degree in electrical engineering from Stanford University, Stanford, CA, USA, in 1990. He has held research positions with the Department of Electrical Engineering, Linköping University, the Information Systems Laboratory, Stanford University, the Katholieke Universiteit Leuven, Leuven, Belgium, and the University of Luxembourg, Luxembourg. From 1996 to 1997, he was the Director of Research with ArrayComm, Inc., a start-up in San Jose, CA, USA, based on his patented technology. In 1991, he was appointed Professor of signal processing with the Royal Institute of Technology (KTH), Stockholm, Sweden. Dr. Ottersten has been Head of the Department for Signals, Sensors, and Systems, KTH, and Dean of the School of Electrical Engineering, KTH. He is the founding Director of the Interdisciplinary Centre for Security, Reliability and Trust, University of Luxembourg. He is a recipient of the IEEE Fourier Technical Field Award, the IEEE Signal Processing Society Technical Achievement Award, the EURASIP Group Technical Achievement Award, and the European Research Council (ERC) advanced research grant twice. He has co-authored journal papers that received the IEEE Signal Processing Society Best Paper Award in 1993, 2001, 2006, 2013, and 2019, and 9 IEEE conference papers best paper awards. He has been a board member of IEEE Signal Processing Society, the Swedish Research Council and currently serves at the boards of EURASIP and the Swedish Foundation for Strategic Research as well as on the ERC Scientific Council. Dr. Ottersten has served as Editor in Chief of EURASIP Signal Processing, and acted on the editorial boards of IEEE Transactions on Signal Processing, IEEE Signal Processing Magazine, IEEE Open Journal for Signal Processing, EURASIP Journal of Advances in Signal Processing and Foundations and Trends in Signal Processing. He is a fellow of IEEE, EURASIP, AAIA, and the Royal Swedish Academy of Engineering Sciences.